Published in final edited form as:
Hippocampus. 2013 September ; 23(9): 751–785. doi:10.1002/hipo.22141.

Quantitative Assessment of CA1 Local Circuits: Knowledge Base for Interneuron-Pyramidal Cell Connectivity

Marianne J. Bezaire and **Ivan Soltesz**
Department of Anatomy and Neurobiology, University of California, Irvine, California 92697-1280, USA

Abstract

In this work, through a detailed literature review, data-mining, and extensive calculations, we provide a current, quantitative estimate of the cellular and synaptic constituents of the CA1 region of the rat hippocampus. Beyond estimating the cell numbers of GABAergic interneuron types, we calculate their convergence onto CA1 pyramidal cells and compare it with the known input synapses on CA1 pyramidal cells. The convergence calculation and comparison are also made for excitatory inputs to CA1 pyramidal cells. In addition, we provide a summary of the excitatory and inhibitory convergence onto interneurons. The quantitative knowledge base assembled and synthesized here forms the basis for data-driven, large-scale computational modeling efforts. Additionally, this work highlights specific instances where the available data are incomplete, which should inspire targeted experimental projects towards a more complete quantification of the CA1 neurons and their connectivity.

Keywords

convergence; divergence; big data; synapses; boutons

1 Introduction

In this assessment, we systematically evaluate available experimental data to quantify the connectivity of GABAergic interneurons and pyramidal cells within the rat CA1. The purpose of this work is to enable the quantitative characterization of the synaptic and cellular components of the circuit in order to form a knowledge base that can be used to construct and constrain data-driven computational models of the CA1 network. The knowledge base used for such models will likely serve other purposes as well; e.g., it can help define the limits of our collective knowledge (see below) and guide future theoretical and experimental studies. It is important to note that the present work is not a review in the conventional sense, as its purpose is not to offer a new synthesis or perspective of the existing literature, and, unlike a review, the current study references previous experimental work solely to drive original calculations to quantify the CA1 network.

Are there sufficient data to assess quantitatively the CA1? Yes and no. Our survey reveals a surprising amount of detailed, quantitative information either directly available or indirectly derivable from existing, published data. However, the data are incomplete. Far from being a deterrent, the incompleteness of the data call for such an assessment: by determining what experimental data are missing, we highlight the specific work necessary to quantify fully the

Corresponding Author: Marianne J. Bezaire, University of California, Irvine, Anatomy & Neurobiology, 192 Irvine Hall, Irvine, CA 92697-1280, 805-368-4956, marianne.case@uci.edu.

connectivity of the CA1. Given the amount of data already published about the CA1, this goal is quite achievable.

The CA1 network is one of the most studied areas in the mammalian brain. Both experimentalists and modelers are interested in the roles played by each interneuron type in the function of the CA1 network. As the field progresses in hypothesizing about and testing the roles of various CA1 interneurons and microcircuits, an idea of the relative abundance of each interneuron and its connections with other neurons has become important. To build a truly data-constrained network model, the assembly of a current knowledge base is not just important, but a requirement.

The knowledge base we have produced here should inspire future projects for two reasons. One, our assessment is a single-frame shot of the state of our collective knowledge. Because of the fast-moving pace of research, it will need to be updated continually in the future. Two, the information would be more accessible in an online database. By publishing our assessment in this form, we hope to lay a framework upon which others can build an online system of sharing and calculating quantitative data. The systematic analysis and development of large, quantitative microcircuit connectivity data described in this paper is an example of how the emerging framework of "Big Data" (Mayer-Schonberger and Cukier, 2013) can be applied to neurobiology. On the other hand, it is important to emphasize that, in many cases, because of the incompleteness of the available data, we were forced to make significant assumptions to complete our calculations. Aware that others may have chosen different strategies from us, we have laid out the paper to facilitate exactly that. Each assumption is stated clearly and explicitly in the text, as well as listed in a table of assumptions. This table may serve as a survey of experimental work necessary to increase the precision of our quantification. We hope to accomplish two ends by laying out our work in this way: one, to maximize our use of the available experimental data and two, to ease the replacement of our assumptions with new experimental data as they become available.

The CA1 hippocampal subfield contains more than 21 types of interneurons (Klausberger and Somogyi, 2008) in addition to pyramidal cells. Decades of observation have produced information about their morphology, intrinsic properties, chemical markers, and connections (Freund and Buzsaki, 1996; Parra et al., 1998). However, quantitative, evidence-based estimates of the number and connectivity of each type have not yet been computed. Therefore, in this work we have calculated the relative numbers and connectivity of the most well known interneuron types, based on existing experimental observations. When performing the calculations, we took advantage of the remarkable diversity of interneurons. Anatomically, interneurons vary in many characteristics: the arborization patterns of the dendrites and axon, the markers expressed (neuropeptides, receptors, calcium-binding proteins) and the layer in which the soma is usually found (Freund and Buzsaki, 1996; Soltesz, 2006; Ascoli et al., 2008). We combined experimental observations about many of these characteristics to arrive at estimates for each interneuron type. We then combined our initial calculations with published light and electron microscopic observations of morphology and synaptic density to estimate the connectivity of each interneuron type.

2 Methods

In this work, we abbreviated some neuron types, the layers of the CA1, and all markers expressed by neurons, as shown in Table 1. Note that the calculations used in this assessment have been organized into a spreadsheet and online database and made available on our website, at http://www.ivansolteszlab.org/quantitativeassessment.html, so that others may easily reproduce or refine the calculations as more experimental data become available.

2.1 Explicit, Forced Assumptions

In the course of the assessment, we sometimes came to a point where not enough data were published to continue with the calculations. In these cases, we usually chose to make what we felt were reasonable assumptions for the purpose of continuing the calculation to reach a rough estimate. Where we made these assumptions, we have clearly documented them. In some cases, we simplified the situation because we felt a reasonable estimate could be made without incorporating all the details or exceptions known for that situation. In other cases, a particular necessary value had not been published, so we picked a reasonable one and continued with the calculations. With each assumption, we marked in the text where it was made, as well as listed and explained it separately in a table (Table 2). In the table, we have noted if any data have been published that are relevant to our assumption.

2.2 Calculation of Neuron Numbers

We calculated cell numbers for the most published interneuron types included in Klausberger and Somogyi, 2008. In determining the relative abundance of each interneuron type, we looked for characteristics that, when combined, uniquely identified a neuron type population. The key attribute that distinguishes the various interneuron types is the axonal arborization pattern, which defines where GABA is delivered on the distinct axo-somato-dendritic domains of postsynaptic neurons. However, for technical reasons, quantitative neuron counts cannot be made based on axonal arborization alone. Such an approach would require that we visualize and count all neurons of a single subtype within CA1 of a given animal, with each and every neuron's axonal arbor visualized and verified as belonging to that particular neuronal subtype, which is not currently experimentally feasible. Consequently, the calculation of neuron numbers was chiefly based on expression of neurochemical markers. Note that electrophysiological properties are also important in the definition of the cell type. The electrophysiological characteristics of the cell types are an integral part of most of the papers on which this work is based, and are therefore implicitly used in the grouping and definition of each cell type.

By necessity, we often considered co-expression of a certain marker combination as a signature of a particular interneuron type. However, not all interneurons of a given type necessarily express markers reliably enough to be detected, so that a calculation of neuron numbers for that type may be low, as noted in the text. Also, for some marker combinations, lesser known neuron types may contribute to the population, such that the calculation overestimates a cell type. For example, calretinin-expressing projection interneurons may inadvertently contribute to the calculation of interneuron-specific I and III cells. These potential issues are noted in discussion of the relevant neuron types within the text, and we have addressed these issues where possible. After completing our analysis, a small percentage of neurons remained undefined; this number represents the leeway on the calculated neuron types plus the contribution of the lesser known neuron types, for which we could not estimate their number.

In some cases, we used marker expression by layer to refine our estimates. For definitions of the hippocampal layers, we followed the descriptions in Andersen et al., 2007, chapter 3, section 3.4.2. While layer position is not sufficient to identify neuron types, quantitative data are often layer-specific and could be used as a guide for differentiating similar neuron types. For example, when estimating the numbers of CCK+ neurons other than basket cells, we assumed CCK+ neurons in the stratum lacunosum-moleculare were perforant path-associated cells, while those in the stratum radiatum were Schaffer Collateral-associated or apical dendritic innervating cells. Mindful that species, strain, sex, and age variations could introduce inconsistencies into our assessment, we tracked these factors for each study we

included. All research to which we refer was performed in rats unless explicitly noted otherwise. Table 3 gives the strains, sexes, ages, and weights of the animals used.

In addition, we tracked the methods employed by the references to obtain the marker expression data used in our assessment. Almost all references employed some form of immunochemistry; a few references also used other methods. The only marker expression reference that did not use immunochemistry was Sik et al. (1994), which instead used NADPH diaphorase histochemistry to determine the presence of nNOS. A few references used additional methods. Fuentealba et al., 2008b and 2010 and Tricoire et al., 2010 used *in situ* hybridization. Price et al., 2005, Tricoire et al., 2010, and Szabo et al., 2012 used single-cell reverse-transcriptase PCR.

To arrive at more detailed estimates, we made assumptions about the marker expression, laminar distribution, and relative abundance of various neuron types. All assumptions are listed in a separate table (Table 2), as well as in the text. In general, we did not account for any gradients or heterogeneity in the distribution of individual neuron types. For example, throughout the calculations we assumed the CA1 was homogenous along the septotemporal axis. We averaged observations made in dorsal and ventral CA1 where available, or in some cases took observations made in the dorsal CA1 to be representative of the entire CA1. We made these simplifications though gradients and heterogeneity in marker expression have been shown for some markers in both principal neurons and interneurons (Kosaka et al., 1987; Nomura et al., 1997a,b; Fuentealba et al., 2010). These simplifications should be revisited in models where dorsal/ventral differences are of interest. Additionally, cellular properties and connectivity can vary as a function of depth within a layer or other factors (Mizuseki et al., 2011; Slomianka et al., 2011; Graves et al., 2012). Therefore, we made these simplifications because not enough information is available to incorporate these characteristics into our estimates, although these factors are important for certain aspects of hippocampal function.

For some interneuron types, there were not sufficient data to calculate cell numbers, so we were unable to include the cell type here. Types that were excluded due to lack of data include large calbindin and RADI cells, as well as potentially other cells that are lesser known and therefore not included within the review of Klausberger and Somogyi, 2008.

2.3 Calculation of Connectivity

For many neuron types, estimates were available of the total boutons per axonal arborization. We multiplied these estimates by the total number of each neuron type as calculated here to get the total number of boutons available for synapsing on postsynaptic neurons. Then we combined these data with the pyramidal cell and interneuron electron microscopy (EM) data to obtain the final convergence and divergence estimates in terms of synapses on a pyramidal cell or interneuron. These calculations allow us to determine the overall connectivity of each neuron type, but do not allow us to calculate the local connection probability. To do so would require knowledge of the bouton distribution within the axonal extent, as well as the density of neurons of each type and their dendritic extents. However, we have still included data on the axonal extent of each neuron type wherever possible.

The total number of synapses onto a pyramidal cell has previously been calculated. Megias et al. (2001) measured dendritic length and synapse density, multiplying the two to calculate the total synapses. They estimated the number of synapses on each type of dendrite across all layers for a pyramidal cell within the dorsal CA1 (Megias et al., 2001). We took this work as the basis for our calculations of synaptic convergence onto CA1 pyramidal cells. There was not sufficient information to calculate the convergence onto each interneuron

type. Instead, we calculated the convergence onto a hypothetical average interneuron to gain a very rough understanding of the possible connectivity among interneurons. This concept of a hypothetical average interneuron provided us with a mechanism to compare our calculations of the GABAergic boutons available to synapse on interneurons with experimental data about synapses on several neurochemical classes of interneuron (Gulyas et al., 1999; Matyas et al., 2004). Given the remarkable diversity of interneurons (Soltesz, 2006), we do not intend for this average to characterize any particular interneuron in the CA1.

3 Results

First, we estimated the number of most types of interneuron as shown in Table 4 and Figures 1 and 2. For those types that had sufficient data, we also calculated their bouton (output synapse) numbers, as well as the bouton distribution as a function of layer and postsynaptic neuron class, to estimate the divergence of each interneuron type (Table 5). Next, we calculated the convergence of each interneuron type and major excitatory afferent type (input synapses) onto pyramidal cells and onto a hypothetical average interneuron.

3.1 Neuron Numbers, Boutons, and Divergence

Here, we began by estimating the total number of neurons in the rat CA1 as 350,000, within the range found for 30 day old Wistar rats (320,000−380,000) (West et al., 1991). GABAergic interneurons constitute 7−11% of all hippocampal neurons (Woodson et al., 1989; Aika et al., 1994). To get a more precise estimate, we calculated the average number of boutons each interneuron would need to have available to synapse on pyramidal cells if the total fraction of GABAergic neurons were 7% or 11%. At 7%, given that CA1 pyramidal cells receive approximately 1,830 GABAergic synapses on their dendrites, somata, and proximal axons (Megias et al., 2001), each interneuron would need to have 24,310 boutons available for synapsing onto pyramidal cells. However, with a fraction of 11%, each interneuron would need only 14,810 boutons to synapse on pyramidal cells, within the range of bouton counts seen for most interneurons. Though neurogliaform family cells have many more boutons, when only the boutons contributing to classical synapses are considered (Olah et al., 2009), the numbers are also within range. Therefore, we generated the following estimates using the interneuronal fraction of 11%, for a total of 311,500 pyramidal cells and 38,500 GABAergic interneurons (note that the 11% interneuronal fraction is listed as an assumption in Table 2).

Note that, for calculating both divergence and convergence as a function of neuron class (pyramidal or interneuron), we needed each interneuron's preference for innervating pyramidal cells over interneurons. For some neuron types, these data have been published. For those types for which the data were not available, we assumed they innervated their postsynaptic targets in the ratio of 92 pyramidal cell synapses to eight interneuron synapses. To arrive at this ratio, we performed the following calculation. We first calculated the average number of GABAergic synapses made onto interneurons (Table 6) using published data about the GABAergic synapses onto various interneuron types (Gulyas et al., 1999; Matyas et al., 2004; Takacs et al., 2008) and our estimated neuron numbers. We weighted the number found on PV+ cells by the calculated number of PV+ basket, bistratified, and axo-axonic cells, the number found on CCK+ basket cells by the number of CCK+ basket cells, the number found on CR+ cells by the total number of IS I and IS III cells, and the number found on hippocampal-septal cells by the number of septally projecting cells to get an average of 1,274 GABAergic input synapses per interneuron (Table 6). We then multiplied this average by the estimated number of interneurons in the CA1 and compared it to the total number of GABAergic synapses on all pyramidal cells in the CA1. We found that GABAergic synapses onto interneurons make up only 8% of all GABAergic synapses in

the CA1, while GABAergic synapses onto pyramidal cells make up the other 92%. Therefore, when the preference for innervating pyramidal cells over interneurons was not reported for a given neuron type, we assumed the ratio was 92:8 pyramidal cells:interneurons (Table 2).

3.1.1 Pyramidal cells

Pyramidal cell numbers: Though CA1 pyramidal cells are increasingly recognized to be more heterogeneous than previously realized (Mizuseki et al., 2011; Slomianka et al., 2011; Graves et al., 2012), in the absence of detailed, quantitative information, we considered them as one homogenous group of 311,500 cells (see assumption in Table 2).

Pyramidal cell boutons and divergence: We calculated the total boutons on a CA1 pyramidal cell axon using the observed axon length and bouton density (Esclapez et al., 1999). Esclapez et al. (1999) provided bouton density measurements as a function of axonal segment branch order for CA1 pyramidal cells. Although the axonal length was computed from an axon fill in a slice, the axon fills were selected from those that appeared to be fully contained within the slice (Esclapez et al., 1999). In a representative CA1 pyramidal axonal arbor, segments of third or fourth order constituted most of the axonal length; therefore we used an average of the bouton densities of the third and fourth order segments (13.56 boutons per 100 μm) multiplied by the average total axonal length (3,732 μm) to obtain a total of 506 boutons per CA1 pyramidal cell within the CA1.

Takacs et al. (2012) recently observed that 39% of local collateral boutons synapse on other pyramidal cells in vivo, so we calculated that each pyramidal cell makes 197 synapses onto other pyramidal cells. We were also interested in the number of synapses made per connection to calculate the divergence, or total number of connections made, onto other pyramidal cells. We assumed that CA1 pyramidal cell local collaterals made one synapse onto each postsynaptic pyramidal cell (Table 2). In a study of pyramidal to pyramidal cell pairs within the CA1 (Deuchars and Thomson, 1996), a pyramidal to pyramidal connection comprising two synapses was found. However, its EPSP amplitude was over twice the average amplitude of the other recorded pairs, so we assumed it was an exception. Therefore, we calculated that each pyramidal cell diverges to contact 197 other CA1 pyramidal cells.

Takacs et al. (2012) also found that CA1 pyramidal cells make 54% of their local synapses onto interneurons. To calculate their divergence onto interneurons, we estimated the number of synapses forming each pyramidal cell to interneuron connection. Biro et al. (2005) observed that a single CA1 pyramidal cell to O-LM cell connection comprised, on average, three synapses. Although some pyramidal cell to basket cell connections in the CA3 were observed to include only one synapse (Sik et al., 1993; Gulyas et al., 1993), current clamp recordings of pyramidal cell to bistratified cell connections in the CA1 revealed a large enough range in EPSP amplitude to suggest that some connections include multiple synapses (Ali et al., 1998). Therefore, we assumed that CA1 pyramidal cells made, on average, three synapses onto each postsynaptic interneuron (Table 2). We then calculated that each CA1 pyramidal cell diverges to innervate 91 interneurons. Aside from the 39% of synapses made onto other pyramidal cells and the 54% made onto interneurons, there are an additional 7% of local synapses made onto unknown targets (Takacs et al., 2012). Therefore, each CA1 pyramidal cell contacts an additional 11 − 35 unknown, local targets.

3.1.2 Neurogliaform family cells—Neurogliaform family cells, including ivy and neurogliaform cells, form the most abundant group of interneurons within the CA1 (for a review, see Armstrong et al., 2012). They often express neuronal nitric oxide synthase

(nNOS), neuropeptide Y (NPY), and α-actinin-2, as well as the nuclear receptor COUP-TFII (Price et al., 2005; Fuentealba et al., 2010). We first calculated the number of COUP-TFII+ cells and then used data about the co-expression of COUP-TFII with nNOS and NPY or α-actinin-2 to estimate the number of ivy and neurogliaform cells. We assumed that all nNOS +/NPY+ cells in the strata oriens, pyramidale, and radiatum were either ivy or neurogliaform cells (Table 2). However, Price et al. (2005) found that, in the stratum lacunosum-moleculare, some non-neurogliaform cells also expressed nNOS or, more rarely, nNOS and NPY. Therefore, in our calculations for neurogliaform cells in the stratum lacunosum-moleculare, we relied on α-actinin-2 expression only.

Though there is known to be a dorsal/ventral gradient in the expression of COUP-TFII, we assumed the expression of COUP-TFII in interneurons dorsally is representative of the whole CA1 (Table 2). Approximately 42% of GABAergic neurons in the CA1 express COUP-TFII (Fuentealba et al., 2010). Conversely, about 98% of COUP-TFII expressing neurons in the CA1 are GABAergic. Combining these two observations (Figure 3), there are roughly 16,500 COUP-TFII expressing neurons in the CA1 and 16,170 COUP-TFII+/GABAergic neurons in the CA1. We combined this estimate of COUP-TFII+ neurons with their experimentally observed laminar distribution (Fuentealba et al., 2010, see their suppl. fig. 1A) to get the total number of COUP-TFII+ neurons per layer, as shown in Table 7. Next, we used these numbers to calculate the number of ivy and neurogliaform cells. Because the assays looked at the coexpression of various markers with COUP-TFII, but not GABA, we performed our calculations on the basis of COUP-TFII+ neurons, rather than GABAergic COUP-TFII+ neurons. However, we considered any neurons expressing nNOS or NPY to be GABAergic.

Ivy cell numbers: Ivy cells express nNOS and NPY (Fuentealba et al., 2008a) but not reelin (Fuentealba et al., 2010; Armstrong et al., 2012). Their somata are generally found in the stratum pyramidale and sometimes in the strata radiatum or oriens (Fuentealba et al., 2010; Somogyi et al., 2012). Not all ivy cells express COUP-TFII (Fuentealba et al., 2010), so nNOS/NPY expression is a better indicator of ivy cells than the presence of COUP-TFII with nNOS and NPY. No other cell type in the stratum pyramidale is known to express both nNOS and NPY, though bistratified cells express NPY (Klausberger et al., 2004; Fuentealba et al., 2008a) and interneuron-specific III cells may express nNOS (Tricoire et al., 2010, in mouse).

From Table 7, there are 5,780 COUP-TFII expressing cells in the stratum pyramidale. Approximately 59% of these cells express nNOS and NPY (Fuentealba et al., 2010, see their suppl. table 2), giving a total of 3,410 COUP-TFII+/nNOS+/NPY+ cells in the stratum pyramidale. It is known that 63% of nNOS+/NPY+ cells in the stratum pyramidale express COUP-TFII (Fuentealba et al., 2010, see their suppl. table 2). Using the logic in Figure 4(a), we determined there are about 5,410 nNOS+/NPY+ cells, the putative ivy cells, in the stratum pyramidale.

We repeated this exercise for nNOS+/NPY+ cells in the stratum oriens. Approximately 34% of the 2,310 COUP-TFII+ cells in the stratum oriens are also nNOS+/NPY+ (Fuentealba et al., 2010, see their suppl. table 2). Though some projection cells may express nNOS (Sik et al., 1994) and double projection cells can express NPY (Klausberger, 2009), no other cell type in the stratum oriens is known to be nNOS+/NPY+. Therefore, we assumed all nNOS+/NPY+ cells in the stratum oriens were ivy cells (Table 2). Using the logic in Figure 4(b), we estimated there are roughly 980 ivy (nNOS+/NPY+) cells in the stratum oriens.

For the ivy cells in the stratum radiatum, we first calculated the number of nNOS+/NPY+ cells. Then we considered that neurogliaform cells may also contribute to the nNOS+/NPY+

cell count in the stratum radiatum, as neurogliaform cells are often found at the border of the stratum radiatum and lacunosum-moleculare (Klausberger and Somogyi, 2008). Ivy cells predominate in the stratum radiatum (Somogyi et al., 2012): coexpression data of NPY and nNOS with reelin, a neurogliaform cell marker (see Armstrong et al. (2012)), showed reelin-expressing cells constituted only 20% of nNOS+/NPY+ cells in the stratum radiatum. Following the logic in Figure 4(c), we determined there are 3,030 nNOS+/NPY+ cells in the stratum radiatum. Applying the observation by Somogyi et al., (2012) of reelin expression in the stratum radiatum, we calculated that 2,420 (80%) of the nNOS+/NPY+ cells are ivy cells (Table 2). We estimated a total of 8,810 ivy cells across strata oriens, pyramidale, and radiatum.

Neurogliaform cell numbers: Neurogliaform cells are found in the stratum lacunosum-moleculare or at the border of the distal stratum radiatum (Vida et al., 1998), and they can express NPY, α-actinin-2, or nNOS (Price et al., 2005; Fuentealba et al., 2010). According to a recent report, there are at least two subsets of neurogliaform cells: those that arise from the MGE and those that arise from the CGE (Tricoire et al., 2010, in mouse). Those cells derived from the MGE are expected to express nNOS and those from the CGE to express COUP-TFII. However, a significant coexpression of COUP-TFII and nNOS has been found for cells in all layers of the CA1 (Fuentealba et al., 2010). Further, there is evidence for a CGE origin for some nNOS+ cells (Tricoire et al., 2010, in mouse; Tricoire and Vitalis, 2012). Therefore, neurogliaform cells do not necessarily cleanly separate into two groups when taking into account both neurochemical identity and origin. This may be due to interspecies differences, a dorsal/ventral gradient in expression, different methods of observation, or other factors. To estimate the expression of nNOS by neurogliaform cells, we calculated the percent of NPY+ cells in the stratum lacunosum-moleculare that co-express nNOS (Fuentealba et al., 2010, see their suppl. table 2). In the stratum lacunosum-moleculare, the fraction of NPY+ cells that also express nNOS ranges from 41% – 85% (Table 8) depending on the combination of neurochemical markers tested in the assay (Fuentealba et al., 2010, see their suppl. table 2). Data about co-expression of nNOS with α-actinin-2 were also available, though not as a function of layer. Overall, 46 − 63% of α-actinin-2+ cells throughout the CA1 expressed nNOS (Price et al., 2005; Fuentealba et al., 2008a, see their Table S2).

A more reliable marker of neurogliaform cells would be NPY or α-actinin-2 (Vida et al., 1998; Ratzliff and Soltesz, 2001; Price et al., 2005). Approximately 71% of neurogliaform cells in the stratum lacunosum-moleculare express α-actinin-2 (Price et al., 2005). In the stratum lacunosum-moleculare, 100% of α-actinin-2+ cells express COUP-TFII, while 45% of COUP-TFII+ cells express α-actinin-2. We calculated the number of α-actinin-2 expressing cells in the stratum lacunosum-moleculare using the logic in Figure 5(a), for a total of 2,150 α-actinin-2+ cells. In the stratum lacunosum-moleculare, α-actinin-2 appears to be a relatively specific marker: α-actinin-2+ cells do not co-express PV, CB, VIP, or CCK (Ratzliff and Soltesz, 2001). Only 2% of α-actinin-2+ cells in that layer express CR, while 43% express NPY (Ratzliff and Soltesz, 2001). Previous work has considered α-actinin-2+ cells in the stratum lacunosum-moleculare as neurogliaform cells (Fuentealba et al., 2010). We assumed that, in the stratum lacunosum-moleculare, 98% of α-actinin-2 expressing cells were neurogliaform cells (the percent of α-actinin-2+ cells that are GABAergic but do not express CR (Ratzliff and Soltesz, 2001); see Table 2). Using the knowledge that 71% of neurogliaform cells express α-actinin-2 (Price et al., 2005) and the logic in Figure 5(b), we calculated there are 2,970 neurogliaform cells in the stratum lacunosum-moleculare. We then included 20% of the nNOS+/NPY+ cells in the stratum radiatum (610 reelin+ cells (Table 2), as calculated above in the ivy cell section), to get a total of 3,580 neurogliaform cells across the strata radiatum and lacunosum-moleculare. Because not all neurogliaform cells express nNOS, there may be even more neurogliaform

cells in the stratum radiatum. However, we did not calculate the number of α-actinin-2+ cells in the stratum radiatum because data were not available about the overlap of α-actinin-2 with COUP-TFII in the stratum radiatum (Fuentealba et al., 2010).

Neurogliaform family cell boutons: Neurogliaform family cells (ivy and neurogliaform cells) are known to have a much higher bouton count than other cell types. For neurogliaform family cells, we averaged two estimates of interbouton length: 2.5 μm (Szabadics and Soltesz, 2009) for ivy cells in the CA3 and 2.3 μm (Armstrong et al., 2011) for neurogliaform cells in the dentate gyrus to get an average of 2.4 μm. Also, 78% of boutons are not involved in classical synapses, instead affecting other neurons via volume transmission (Olah et al., 2009, in somatosensory cortex). Therefore, we subtracted 78% of boutons from the total bouton count to determine the number of classical synapses made by each cell. However, the boutons not participating in the classical synapses are still involved with volume transmission (Olah et al., 2009, in somatosensory cortex) and are therefore functionally relevant. Their contribution should be considered in any theoretical or computer model that includes ivy and neurogliaform synapses. For both neurogliaform and ivy cells, we assumed they made 10 classical synapses per connection (Table 2). This assumption is based on the observation that neurogliaform cells in the somatosensory cortex were predicted to make 10 synapses per connection, though the status of those synapses as classical (with a corresponding postsynaptic element) was not confirmed (Tamas et al., 2003).

Ivy cell boutons: The axonal extent of the ivy cells is 0.75 mm in the medio-lateral direction and 1.31 mm in the rostro-caudal direction (Fuentealba et al., 2008a). Their total axonal length was calculated by comparison with a bistratified cell axonal arbor. By measuring the relative axonal lengths of ivy and bistratified cells within a 100x100x70 μm volume surrounding the soma, ivy cells were found to have an axon length 2.2 times that of bistratified cells (Fuentealba et al., 2008a). A complete bistratified cell axon had previously been measured as 78,800 μm; therefore, we calculated a total ivy cell axon length of 176,760 μm. We calculated the total bouton count, at a density of one per every 2.4 μm, as 73,650. Considering only 22% of synapses make classical synapses (Olah et al., 2009), we calculated 16,200 boutons available for classical synapses. We assumed ivy cells made 10 classical synapses on each postsynaptic cell (Table 2). Therefore, they diverge to innervate 1,620 cells. Their relative preference for synapsing on pyramidal cells versus interneurons is not known, so we used the ratio of 92:8 as discussed above (Table 2). We calculated that they contact 1,490 pyramidal cells and 130 interneurons. Ivy cells make most of their synapses in the strata oriens and radiatum (Fuentealba et al., 2008a; Klausberger, 2009). Different studies have found different distributions for ivy cell axons, as shown in Table 9. We took the average of two studies (Fuentealba et al., 2008a; Szabo et al., 2012), assuming that ivy cells make 40% of their synapses in the stratum oriens and 50% in the stratum radiatum.

Neurogliaform cell boutons: A neurogliaform cell filled within the confines of a 400 μm slice has more boutons (13,000) than a complete fill of a basket cell axon (10,000) (Halasy et al., 1996; Vida et al., 1998). Also, within an equivalent volume, neurogliaform cell axons have a release probability about five to six times that of basket cells (Olah et al., 2009, in somatosensory cortex). Therefore, each neurogliaform cell has roughly 60,000 boutons. Because 78% of boutons are not involved in classical synapses (Olah et al., 2009, in somatosensory cortex), we determined 13,200 boutons were available for synapses. As we assumed neurogliaform cells make 10 classical synapses per connection (Table 2), their divergence was calculated as 1,320 cells. We assumed they innervate pyramidal cells and

interneurons in a 92:8 ratio (Table 2) for a total of 1,214 pyramidal cells and 106 interneurons.

Neurogliaform axons concentrate around the cell in a tight, radially distributed cloud. The axonal extent of neurogliaform cells was found to be 0.5 mm in the mediolateral axis and 1.2 mm in the septotemporal axis (Fuentealba et al., 2010). Given the total number of boutons and calculated bouton density, we calculated the total axonal length as 144,000 μm. The axons are mostly found within the stratum lacunosum-moleculare (Price et al., 2005). However, as some neurogliaform cells are found within the stratum radiatum (see above), we assumed the distribution of boutons across the strata radiatum and lacunosum-moleculare matched the distribution of somata across those two layers (83% in the stratum lacunosum-moleculare, 17% in the stratum radiatum).

3.1.3 SOM+ Cells—SOM+ cells include O-LM cells and several projection cells (Maccaferri, 2005; Klausberger and Somogyi, 2008), as well as conventional bistratified cells, which will be calculated in the PV+ cell section. Many of the projection cells have a local axonal arborization consisting of boutons primarily in the strata radiatum and oriens. These include double projection cells that project to the septum and subiculum, so-called back-projection cells that project to the CA3 and dentate gyrus, and oriens-retrohippocampal projection cells that target the subiculum (Klausberger and Somogyi, 2008). A projection cell targeting both the CA3 and the subiculum has also recently been discovered (Jinno, 2009, in mouse).

About 12% of GABAergic neurons in the CA1 express SOM (Kosaka et al., 1988). Applying this fraction to the calculation for GABAergic neurons gave 4,620 SOM+ neurons. About 89% of these cells are located in the stratum oriens (Table 10) (Kosaka et al., 1988; Nomura et al., 1997b), a total of 4,110 SOM+ GABAergic cells in the stratum oriens.

O-LM Cells: O-LM cells, which express SOM and mGluR1α (Ferraguti et al., 2004), are found in the stratum oriens (Klausberger and Somogyi, 2008). Roughly 40% of SOM+ cells in the stratum oriens are O-LM cells (Ferraguti et al., 2004), giving a total of 1,640 O-LM cells.

Double Projection Cells: Of the SOM+ cells in the stratum oriens, 23% project to the medial septum (Jinno, 2009, in mouse), a total of 950 septally projecting SOM+ cells. Of the cells projecting to the medial septum, 80% are CB+ (Toth and Freund, 1992; Gulyas et al., 2003; Jinno, 2009). The double projection cells, which project both to the medial septum and to the subiculum, are known to express CB and SOM (Toth and Freund, 1992; Somogyi and Klausberger, 2005; Jinno et al., 2007); some also express mGluR1α, M2R, PV, or NPY (Jinno et al., 2007). We assumed all septally projecting, SOM+/CB+ cells were double projection cells (Table 2), for a total of 760 double projection cells.

Other Septally Projecting Cells: Subtracting the SOM+/CB+ double projection cells from the total of septally projecting cells, we were left with a subset of 190 SOM+/CB-, septally projecting cells. This subset likely constitutes another group of septally projecting cells. Katona et al. (1999a) suggested that so-called back-projection cells, which are not known to express CB but often express SOM (70%, see Jinno, 2009), can project to the septum, in addition to projecting to the CA3. The observation that 18% of septally projecting cells express CR may also be relevant, as it has not been shown that double-projection cells express CR (Jinno, 2009). There is also a subset of SOM+ cells that are weakly M2R+ and may project to the septum, but this subset does not appear to express CR (Hajos and Mody, 1997; Ferraguti et al., 2005). For now, we consider the subset of 190 SOM+/CB- septally projecting cells in our calculations, noting that this cell type may also be the so-called back-

projection cells or a subset of M2R+ septally projecting cells. In addition to these multiple subsets of SOM+ septal projection cells, there may be another small subset of septally projecting cells that are SOM- (Jinno et al., 2007). We do not attempt to identify or include those cells.

Oriens-Retrohippocampal Cells: About 34% of SOM+ cells in the stratum oriens express CB, a total of 1,400 cells (Gulyas et al., 2003). Like double projection cells, oriens-retrohippocampal cells can be SOM+/CB+ but may also express M2R (Jinno et al., 2007). We subtracted the double projection cells from the SOM+/CB+ population in the stratum oriens, leaving 640 other SOM+/CB+ cells, which we assumed were oriens-retrohippocampal cells (Table 2).

Other SOM+ Cells: Other stratum oriens cells also express SOM (Jinno, 2009). Subtracting the estimates for O-LM, oriens-retrohippocampal, double projection, and other septally projecting cells from the total number of SOM+ cells left 880 SOM+ cells unidentified. Most of these are likely to be bistratified cells, which express SOM and PV (Klausberger et al., 2004; Baude et al., 2007) and are sometimes located in the stratum oriens (Baude et al., 2007); they will be calculated in the PV+ cell section.

O-LM cell boutons: The axonal extent of O-LM cells is rather compact, only 500 μm in the medio-lateral direction and 840 μm in the septo-temporal direction (Sik et al., 1995). O-LM cells have a local axonal length of 62,490 μm and a bouton density of 26.6/100 μm (Sik et al., 1995). We calculated a local CA1 bouton count of 16,370 (Sik et al., 1995). A light microscopy study of O-LM to pyramidal cell connections showed a range of three to 17 potential synapses per connection (Maccaferri et al., 2000). We took the average of 10 synapses per connection, giving a divergence of 1,637 cells (Table 2). There are 74% of O-LM cell synapses made onto non-GABAergic cells, while only 9% are made on GABAergic cells and 17% are unidentifiable (Katona et al., 1999a). Of the known synaptic targets, the ratio was 89% of synapses made on pyramidal cells to 11% of synapses made on interneurons (Katona et al., 1999a) for a total innervation of 1,457 pyramidal cells and 180 interneurons. Within the CA1, most of the O-LM cell boutons are found in the stratum lacunosum-moleculare, though a variable amount can be found in the stratum oriens. Sik et al. (1995) found 93% of axon collaterals in the stratum lacunosum-moleculare and 7% in stratum oriens.

Other SOM+ cell boutons: The other projection cells of the stratum oriens with local axons in the CA1 usually innervate the strata radiatum and oriens. In one case, a so-called back-projection cell made 25,000 synapses in the hippocampus (Sik et al., 1994). Of the axon length within the hippocampus, 24.3% remained within the CA1, giving an estimate of 6,080 boutons in the CA1 (Sik et al., 1994). Here, we assumed the other projection neurons with local axon collaterals also had a similar number of boutons in the CA1 (Table 2). For each projection cell with axons in strata radiatum and oriens, we assumed their local boutons were distributed similarly as bistratified cells (Table 2), between the stratum oriens and radiatum, with 58% of their length in the oriens and 42% in the stratum radiatum (following a bistratified cell with its soma in the stratum oriens, from Sik et al. (1995). As the few collaterals within the stratum pyramidale did not exhibit significant numbers of boutons, we were concerned only with the relative proportions in the oriens and radiatum.

For some types of SOM+ cells, information was available about their relative preference for synapsing on pyramidal cells or interneurons. Oriens-retrohippocampal cells send 96% of their boutons to pyramidal cells (Jinno et al., 2007). Jinno et al. (2007) also found that double projection cells send 86% of their local boutons to pyramidal cells and 14% to interneurons, whereas Takacs et al. (2008) found that, of the known local targets of septally

projecting cells, 97% are on pyramidal cells and 3% are on interneurons. We averaged these two data points to calculate that double projection cells make 92% of their local targets on pyramidal cells and 8% on interneurons. Additionally, there appears to be a subset of septally projecting cells that target interneurons locally (Gulyas et al., 2003). It is possible that interneuron-specific septally projecting cells constitute the other group of septally projecting cells mentioned above. This other group is CB- and may align with the 18% of septally projecting cells seen to express CR (Jinno, 2009).

For each of the SOM+ cell types, we assumed the cells contacted their postsynaptic targets with 10 synapses each (Table 2). Because we assumed the same bouton counts for double projection, so-called back projection, and oriens-retrohippocampal cells, they all had a calculated divergence of 608 cells. Their preference for innervating pyramidal cells differed, however. Double projection cells may innervate 559 pyramidal cells and 49 interneurons, while oriens-retrohippocampal cells innervate 584 pyramidal cells and 24 interneurons.

3.1.4 Parvalbumin expressing cells—Approximately 26% of GABAergic neurons in the CA1 express PV (Kosaka et al., 1987). Given our previous calculation of 38,500 GABAergic cells in the CA1, 10,010 PV+ GABAergic cells reside in the CA1. These include the PV+ basket cells, bistratified cells, and axo-axonic cells. Also, up to one third of O-LM cells (Varga et al., 2012, in mouse) and double projection cells (Jinno et al., 2007) express PV, but at a weaker level (but see Ferraguti et al., 2004, where up to 75% of mGluR1α+/SOM+ cells in the stratum oriens also expressed PV). Subtracting one third of the O-LM and double projection cells from the total gave 9,210 remaining PV+ cells.

While 64.5% of PV+ cells are located in the stratum pyramidale, a substantial number reside in the stratum oriens (30%, see Table 11) (Kosaka et al., 1987; Nomura et al., 1997b). Baude et al. (2007) gave relative percentages of PV+ basket, bistratified, and axo-axonic cells in the stratum pyramidale. We assumed the ratio held for the other layers to calculate the number of cells of each type in each layer, for a total of 5,530 PV+ basket cells, 2,210 bistratified cells, and 1,470 axo-axonic cells (Table 12). Note that this number of bistratified cells does not include any contributions from the GABAergic projection cells in the stratum oriens that also have boutons in the strata radiatum and oriens and, in the case of double projection cells, occasionally express PV (Jinno et al., 2007).

PV+ basket cell boutons: The extent of the PV+ basket cell axon was found to be 1,185 μm in the septo-temporal direction and 1,042 μm in the medio-lateral direction (Sik et al., 1995). The total axon length was 46,180 μm (Sik et al., 1995). At a density of 22.6 boutons per 100 μm, the estimated total bouton count per PV+ basket cell was 10,440 (Sik et al., 1995). Most of the boutons were found within the pyramidal layer, with few found in the strata oriens or radiatum (Sik et al., 1995). Though the observed number of basket cell synapses per connection varies from two to 12 (Buhl et al., 1994a; Sik et al., 1995; Buhl et al., 1995; Halasy et al., 1996; Foldy et al., 2010, in mouse), here we took PV+ basket cells to make about 11 synapses on each pyramidal cell (Foldy et al., 2010, in mouse). However, PV+ basket cells have been shown to make connections comprising single or very few synapses on other PV+ interneurons (Sik et al., 1995) (but see Cobb et al. (1997), where a basket cell innervated a bistratified cell with 12 synapses) so we assumed they made only one synapse on all connections with other interneurons (Table 2). Sik et al. (1995) found PV+ basket cells connect with pyramidal cells and other PV+ cells with equal probability, which we took to mean in proportion to the number of each cell type. Therefore, we calculated each PV+ basket cell contacts 1,014 other cells, 943 pyramidal cells and 71 other interneurons.

Bistratified cell boutons: Bistratified cells project to the strata oriens and radiatum (Klausberger, 2009). A range of values has been found for the number of boutons present on

each bistratified cell. Pawelzik et al. (2002) found a mean of 4,000 boutons, in contrast to an earlier finding of 15,970 boutons within the CA1 for a bistratified cell with its soma in the oriens (Sik et al., 1995). Additionally, Halasy et al. (1996) found that a bistratified cell axon within a 400 μm slice contained 8,752 boutons; therefore, the finding of 15,970 boutons in a complete axon within the CA1 seems likely. The bistratified cell observed by Sik et al. (1995) had a local axonal length of 76,040 μm and a bouton density of 21.0 boutons per 100 μm.

Bistratified cells make 10−11 synaptic contacts with each cell they innervate (Klausberger et al., 2004) (but see Buhl et al. (1994a);Miles et al. (1996), where five to nine were found). Therefore, each bistratified cell diverges to contact approximately 1,597 cells. Because the relative preference for synapsing on pyramidal cells was not given, we assumed (Table 2) that bistratified cells synapse on pyramidal cells and interneurons in a 92:8 ratio, for a total divergence of 1,469 pyramidal cells and 128 interneurons.

Laminar distribution data for the bistratified cell was available from both Pawelzik et al. (2002) and Sik et al. (1995); an average was calculated from the two references (Table 13) such that 51% of collaterals were found in the stratum oriens, 7% in the pyramidale, and 42% in the radiatum. Qualitative observations of laminar axonal distribution were also available (Fuentealba et al., 2008a; Halasy et al., 1996). The medio-lateral extent of the axon was 1.15 mm, and rostro-caudally it was 1.53 mm (Klausberger et al., 2004).

Axo-axonic cell boutons: An axo-axonic cell had an elliptically shaped axonal arbor, with a 600 by 850 μm extent (Li et al., 1992). Each axo-axonic cell had multiple rows of boutons, where each row corresponded to the synapses made on one postsynaptic axon. Each row contained two to 10 boutons (Li et al., 1992), with an observed divergence of one axo-axonic cell onto 1,200 pyramidal cells (Li et al., 1992). Therefore, we calculated that each axo-axonic cell has 2,400 − 12,000 boutons and assumed an average of 7,200 boutons per axo-axonic cell (Table 2). Axo-axonic cells appear to contact only pyramidal cells (Buhl et al., 1994a,b).

3.1.5 CCK Expressing Cells—About 12% of the GABAergic neurons in the CA1 express cholecystokinin (CCK) (Kosaka et al., 1985) a total of 4,620 CCK+ GABAergic neurons in the CA1. CCK+ cells usually express cannabinoid receptor type 1 (CB1R) (Katona et al., 1999b; Cope et al., 2002) and often express vasointestinal protein (VIP) (Somogyi et al., 2004), vesicular glutamate transporter 3 (VGLUT3) (Somogyi et al., 2004), or sometimes calbindin (CB) (Cope et al., 2002; Somogyi et al., 2004). The presence of CB1R is generally an indicator of a CCK+ cell (Katona et al., 1999b). Therefore, CB1R expression data may be useful as a confirmation of the total number of CCK+ cells. Given the overlap of CCK and CB1R expression (Katona et al., 1999b) in the somata of CA1 interneurons (Figure 6), we determined that there are 5,400 CB1R+ cells in the CA1. CB1R may be a more reliable indicator of CCK+ cells than CCK expression itself, so we based the rest of our CCK+ cell calculations on a total of 5,400 cells rather than 4,620 cells. However, we did not have detailed laminar distribution or marker expression overlap data for the CB1R+ cells, so we used the corresponding fractions from CCK+ cell studies.

CCK+ cell types include CCK+ basket cells, Schaffer Collateral-associated (SCA) cells, apical dendritic innervating (ADI) cells, and perforant path-associated (PPA) cells. ADI and SCA cells reside mostly in the stratum radiatum (Cope et al., 2002; Klausberger et al., 2005; Klausberger and Somogyi, 2008). PPA cells are found at the border of strata radiatum and lacunosum-moleculare (Somogyi and Klausberger, 2005; Klausberger and Somogyi, 2008). PPA cells are also known as R-LM cells because their cell bodies are generally found near

the stratum radiatum while their axons innervate the stratum lacunosum-moleculare (Hajos and Mody, 1997).

The relative frequency of each of these cell types is unknown. To estimate the number of CCK+ basket cells, we used data about the synaptic convergence of basket cells onto pyramidal cells. Foldy et al. (2010, in mouse) found that PV+ basket cells make about twice as many total synapses onto pyramidal cell somata as do CCK+ basket cells. However, CCK + basket cell boutons are known to occur more frequently proximal to the soma (Foldy et al., 2010, in mouse), as evidenced by Wyeth et al. (2010), who found a ratio of 13.1:10.9 for PV:CCK boutons in the whole pyramidal cell layer of the mouse CA1. We averaged these two estimates to obtain a ratio of 1.6:1 PV:CCK boutons onto pyramidal cells. We assumed this ratio also held for the total number of PV+ basket cell and CCK+ basket cell boutons in the CA1 (Table 2). Because there are approximately 5,520 PV+ basket cells with 10,440 boutons each, the total number of PV+ basket cell boutons in the CA1 is 57.7 million. Therefore, we calculated the total number of CCK+ basket cell boutons as 36.0 million. As CCK+ basket cells may have about 10,000 boutons each (see synapse calculations below), we calculated a total of 3,600 CCK+ basket cells.

Using data from Pawelzik et al. (2002), we determined the laminar distribution of CCK+ cells (Table 14) and estimated the relative abundance of each type of CCK+ cell in each layer. We included marker coexpression data from Somogyi et al. (2004) to solve for the populations of CCK+/CB+, CCK+/VIP+, CCK+/VGLUT3+, and CCK+only cells in each layer, which we used to refine our estimates by cell type.

We assumed (Table 2) the CCK+ basket cells were found in all layers of the CA1 (including the stratum lacunosum-moleculare, see Vida et al., 1998 and Elfant et al., 2008), SCA and ADI cells in the stratum radiatum, and PPA cells in the stratum lacunosum-moleculare (Table 2) (Klausberger and Somogyi, 2008). We assumed some lesser-known CCK+ cell types were found only in the strata oriens and pyramidale (Table 2). The lesser-known types include CCK+ quadrilaminar, CCK+ bistratified cells (different from SCA cells), and CCK+ SO-SO cells, so called because both their axons and dendrites remain in the stratum oriens (Pawelzik et al., 2002). In addition, some of the CCK+ basket cells found in the stratum oriens may be horizontal basket cells (Klausberger et al., 2005).

Since CCK+ basket cells have not been shown to express CB (Cope et al., 2002; Somogyi et al., 2004), we assumed none of the CCK+/CB+ cells were basket cells (Table 2). We considered CCK+/CB+ cells in the stratum lacunosum-moleculare as PPA cells, CCK+/CB+ cells in the stratum radiatum as SCA or ADI cells, and CCK+/CB+ cells in the strata oriens and pyramidale as the lesser-known types mentioned above (Table 2). Note that PPA and SCA cells are both often found straddling the border of the strata radiatum and lacunosum-moleculare, so the laminar-based calculations for these CCK+ cell types will only give a rough approximation of each type.

We assumed all the CCK+/CB- cells in the strata oriens and pyramidale were CCK+ basket cells, including CCK+/VIP+ cells, CCK+/VGLUT3+ cells, and CCK+only cells (Table 2). In the strata radiatum and lacunosum-moleculare, we assumed all the CCK+/VIP+ and CCK +/VGLUT3+ cells were basket cells. However, Klausberger et al. (2005) showed that ADI cells can express VGLUT3 and a high concentration of VGLUT3+ boutons has been found at the border of the strata radiatum and lacunosum-moleculare, suggesting that PPA or SCA cells may also express VGLUT3 (Somogyi et al., 2004) (Table 2). After counting the CCK+/ VIP+ and CCK+/VGLUT3+ cells in the strata radiatum and lacunosum-moleculare, there were still an additional 430 CCK+ basket cells to be assigned, which we assumed to be CCK +only cells. Next, we assumed all of the non-basket cells in the stratum lacunosum-

moleculare were PPA cells (Table 2). Of the non-basket cells in the stratum radiatum, we assumed the SCA and ADI each made up half the balance (Table 2). This led to an estimate of 65% of SCA cells being CB+, though only 32% have been observed to be CB+ experimentally (Cope et al., 2002). The numbers of each CCK+ cell type are given in Table 15.

CCK+ basket cell boutons: Comparably less information is available about CCK+ basket cell axonal arbors than PV+ basket cell axons. Axonal extent, total length, and bouton density were generally not reported, though the proximal-distal extent of a CCK+ basket cell axon was found to be 1 mm (Vida et al., 1998).

The study of stratum radiatum basket cells (presumably CCK+, Table 2) showed that a basket cell axon within a 400 μm slice contained almost 8,000 boutons (Vida et al., 1998). We assumed (Table 2) the same bouton distribution as for the PV+ basket cells (20% more boutons outside the slice, as in Halasy et al., 1996), so the overall bouton count for that cell is likely around 10,000. Though the observed number of basket cell synapses per connection varies from two to 12 (Buhl et al., 1994a; Sik et al., 1995; Buhl et al., 1995; Halasy et al., 1996; Miles et al., 1996; Foldy et al., 2010, in mouse), here we took CCK+ basket cells to make about eight synapses per connection (Foldy et al., 2010, in mouse). It is not known whether CCK+ basket cells make fewer synapses in their connections with other interneurons (as PV+ basket cells do), so we assumed they also made eight synapses per connection with other interneurons (Table 2). This gave a divergence of 1,250 cells: 1,150 pyramidal cells and 100 interneurons assuming the 92:8 ratio of innervation (Table 2). The average laminar distribution of boutons across several CCK+ basket cells was shown to be 19% in the stratum oriens, 60% in the stratum pyramidale, 20% in the stratum radiatum, and 1% in the stratum lacunosum-moleculare (Pawelzik et al., 2002).

SCA cell boutons: The axonal length and bouton density of SCA cells has not been reported. The proximal-distal extent of the axon was found to be 1.1 mm (Vida et al., 1998). A 400 μm slice contained 6,000 boutons (Vida et al., 1998). By comparison, a bistratified cell in the middle of a 400 μm slice had an axon with almost 8,800 boutons (Halasy et al., 1996), but the full, local axonal arbor of another bistratified cell had 15,970 boutons overall (Sik et al., 1995), suggesting that the bouton distribution of bistratified cells extends significantly beyond the confines of a 400 μm slice. Therefore, we assumed the SCA cell axon was distributed similarly and also had only 50% of its boutons within the confines of the 400 μm slice (Table 2); we calculated a complete axon as having approximately 12,000 boutons. SCA cells make approximately six synapses per connection (Vida et al., 1998), so they may contact roughly 2,000 cells. We assumed they contact pyramidal cells and interneurons in a ratio of 92:8 for a total of 1,840 pyramidal cells and 160 interneurons. SCA cells preferentially synapse in the stratum radiatum (Vida et al., 1998; Szabo et al., 2012), with an average distribution of 82% of axons in the stratum radiatum. Table 16 shows the different laminar distributions that have been observed for SCA cells.

ADI cell boutons: No quantitative information has been reported about ADI cell axons. ADI cell boutons are known to innervate the main apical dendrite of pyramidal cells in preference to the oblique dendrites (Klausberger et al., 2005; Klausberger, 2009). If ADI cells gave rise to one tenth of the 111 GABAergic synapses on the distal main apical dendrite of the pyramidal cells (Megias et al., 2001), each of the 390 ADI cells would need approximately 8,870 boutons.

PPA cell boutons: Though a 400 μm slice was found to contain 8,000 boutons, over half of them were positioned outside the CA1 (Vida et al., 1998). We used the same logic as with the SCA cell to estimate a total of 16,000 boutons (Table 2). Considering half of the boutons

as being within the CA1 (Vida et al., 1998) gave a total of 8,000 boutons. PPA cells are thought to make six synapses per connection as seen with SCA cells (Vida et al., 1998), for a divergence of 1,333 cells. We assumed they followed the ratio of 92:8 for innervation, for a total divergence of 1,227 pyramidal cells and 106 interneurons (Table 2).

3.1.6 Interneuron Specific Cells—Interneuron specific (IS) cells only synapse on other interneurons, avoiding the pyramidal cells, and they often express calretinin (CR), VIP, or enkephalin (ENK) (Acsady et al., 1996a,b; Gulyas et al., 1996; Fuentealba et al., 2010). Recently, they have been shown to express COUP-TFII as well (Fuentealba et al., 2010). IS cells can be further divided into multiple categories. One type, known as the IS III cell, expresses both CR and VIP and has axons projecting to the stratum oriens and alveus (Acsady et al., 1996b; Gulyas et al., 1996). A second type, known as the IS II cell, has axons targeting the stratum radiatum and dendrites in the stratum lacunosum-moleculare (Acsady et al., 1996b; Gulyas et al., 1996). This type is known to express VIP but has not been shown to express CR (Somogyi and Klausberger, 2005). A third, broad category known as IS I includes cells with dendrites spanning all layers and axons targeting the stratum radiatum, and perhaps also the stratum oriens (Acsady et al., 1996b; Gulyas et al., 1996). These cells generally express CR, though a subset of them do not (Acsady et al., 1996a). Additionally, a subset of VIP+ cells in mice has been found to express nNOS as well; this subset has axonal and dendritic projection patterns resembling those of an IS III cell (Tricoire et al., 2010, in mouse).

We used data about the coexpression of COUP-TFII with other markers to calculate the number of IS cells. Because some non-IS cells express ENK (Price et al., 2005), we did not consider the presence of ENK to indicate interneuron-specific cells. Instead, we characterized IS cells as those that express CR or VIP (Table 2) (Fuentealba et al., 2010). We used information about the co-expression of CR, VIP, and COUP-TFII (Fuentealba et al., 2010), along with our earlier calculation of COUP-TFII cells per layer, to determine the number of CR or VIP positive cells in each layer (Table 17). We looked at three combinations of marker expression which we took to represent specific IS cell types. We assumed CR+/VIP- cells were IS I cells, CR-/VIP+ cells were IS II cells, and CR+/VIP+ cells were IS III cells (Table 2). This may underestimate the number of IS I cells, since not all of them express CR (Acsady et al., 1996a). Using the logic in Figures 7, 8, and 9, we determined the number of CR+/VIP-, CR-/VIP+, and CR+/VIP+ cells in each layer. Considering some basket cells also express VIP, we subtracted the number of CCK+/VIP+ basket cells, assuming the remaining VIP+ cells were IS cells (Table 2). For each layer, we removed an equal fraction of VIP+ cells (the CCK+/VIP+ basket cells) from the CR-/VIP+ and CR+/VIP+ populations. Note that 18% of septally-projecting cells express CR (Jinno, 2009); this number may align with the 190 SOM+/CB- septally projecting cells that are not double projection cells (calculated above). We subtracted these 190 cells from the CR+/VIP- population of cells in the stratum oriens to obtain an estimate for each IS cell type in each layer (Table 18).

IS cell boutons: Bouton counts of the IS cells were not available, probably due to the difficulty of determining an average bouton density for their axon collaterals. The bouton density of IS cells varies significantly along the axons (Acsady et al., 1996a). This variability in bouton density, with large lengths of axon in which few boutons are found, interspersed with sections of high bouton density, may arise because of these interneurons' selectivity in only synapsing on other interneurons (Acsady et al., 1996a).

3.1.7 Other cells—Several cell types remain for which we have not estimated their number. Here, we provide a crude estimate of number for several types given the limited information we have about them. However, we do not include the estimates made in this

section in our final count in the summary section, because the estimates are likely to contain multiple cell types and may overlap with cell populations already counted.

We have not yet addressed a few of the cell types found in the stratum radiatum. These include large calbindin cells (Klausberger and Somogyi, 2008) and radiatum- and dentate-innervating (RADI) cells (Fuentealba et al., 2010), which both express CB. Freund and Buzsaki (1996) suggested 10% of GABAergic cells in the CA1 express calbindin (CB), for a total of 3,850 CB+ cells (Table 2). We subtracted the previously calculated CB+ cells (CCK+/CB+ cells and SOM+/CB+ cells) from this total, for a remainder of 1,230 CB+ cells across all layers. This represents an upper bound on the large calbindin and RADI cells. They are likely to number much fewer, because the remaining CB+ cells in the strata oriens and pyramidale may actually include some of the other cell types calculated above, for which their CB expression was unknown.

There are additional projection cells that we have not calculated. So-called back projection cells project to the CA3 and dentate gyrus and are known to express nNOS (Sik et al., 1994). They may also express SOM (Katona et al., 1999a) and may even project to the septum (see Other Septally Projecting Cells above). Unfortunately, not enough information is known about so-called back projection cells to estimate their relative abundance or even to consider them as a distinct cell type.

There are also other projection cells that target the subiculum. We performed a rough calculation to gain an idea of the cells projecting to the subiculum, including the radiatum-retrohippocampal cells and the trilaminar cells. To do this, we combined experimental data with the above calculations for double projection and oriens-retrohippocampal cells. Both double projection and oriens-retrohippocampal cells project to the subiculum (Klausberger and Somogyi, 2008). We assumed these two cell types constituted the entire population of SOM+, subicular-projecting cells, a total of 1,400 cells (Table 2). Since 50% of cells in the CA1 projecting to the subiculum are SOM+ (Jinno et al., 2007; Jinno, 2009), we calculated that a total of 1,400 SOM- cells project to the subiculum. These are likely to include trilaminar cells in the stratum oriens and radiatum-retrohippocampal cells in the stratum radiatum, both of which project to the subiculum and are not seen to express SOM. However, as both of these cell types are somewhat rare, it is unlikely that they comprise the entire group of SOM- subicular projecting cells.

No data were available to break down our estimate of trilaminar and radiatum-retrohippocampal cells into an estimate for each cell type or even by layer. Once more data become available about the laminar distribution and total number of subicular projecting cells, further identification may be possible. Radiatum-retrohippocampal projection cells have not been found to express any of the major neurochemical markers, such as SOM, VIP, nNOS, CCK, CB, PV or CR, nor any particular receptors (Jinno et al., 2007; Jinno, 2009), though 80% of them express COUP-TFII (Fuentealba et al., 2010). Therefore, it is difficult to make any estimation for this type of cell. Of note, a study marking neurons that project to the granular retrosplenal cortex found that a significant portion of the axons originated from GABAergic neurons at the border of the strata radiatum and lacunosum-moleculare (Miyashita and Rockland, 2007). Most of the cells were found to be negative for the major neurochemical markers, though a small percentage expressed M2R (Miyashita and Rockland, 2007). Some of these neurons may be radiatum-retrohippocampal cells. Also, within the strata radiatum and lacunosum-moleculare, about 5% of subicular projecting cells were negative for all tested markers (Miyashita and Rockland, 2007); these cells may correspond to some or all of the putative radiatum-retrohippocampal cells.

In both the strata oriens and radiatum, approximately half of subicular projecting cells were M2R+. These M2R+, subicular projecting cells are the putative trilaminar cells that locally innervate stratum pyramidale in addition to the strata radiatum and oriens (Sik et al., 1995; Ferraguti et al., 2005; Klausberger and Somogyi, 2008). However, trilaminar cells are considered somewhat rare, so it is not clear whether they make up the entire M2R+, subicularly projecting population. Trilaminar cells are also mGluR8-decorated (Ferraguti et al., 2005); however, there is not enough information about the prevalence of mGluR8-decorated cells to base any calculations on that property.

In addition, a population of ENK expressing cells in the stratum radiatum has recently been found (Fuentealba et al., 2008b). This cell type projects to the subiculum as well; 11.3% of subicular projecting interneurons in the CA1 expressed ENK (Fuentealba et al., 2008b). Given our calculations of subicular projecting interneurons above (2,800), approximately 320 subicular projecting cells may express ENK.

Trilaminar cell boutons: There was sufficient information about trilaminar cells to estimate their divergence. Trilaminar cells innervate mainly the stratum oriens and stratum radiatum, but also the stratum pyramidale (Klausberger, 2009). They should be considered distinct from other projection cells whose axons mainly ramify in the strata radiatum and oriens, the cell types formerly known as oriens-bistratified cells (Maccaferri et al., 2000). Of the synapses made within the CA1, a trilaminar cell made 70% of its synapses in the stratum radiatum, 17% in the stratum pyramidale, and 13% in the stratum oriens (Sik et al., 1995). The observed axonal length and bouton density suggested the trilaminar cell had 15,800 boutons within the hippocampal formation, with 15,440 boutons in the CA1 (Sik et al., 1995). A trilaminar cell from a different study made 40% of its synapses on pyramidal cells, while 60% were made onto interneurons (Ferraguti et al., 2005). The trilaminar cell observed in Ferraguti et al. (2005) had a more extensive axonal projection to the subiculum and most of its axon collaterals ramified in the stratum oriens, rather than the stratum radiatum, as compared to the trilaminar cell in Sik et al. (1995). Note that the trilaminar cell from Ferraguti et al., 2005 was considered as an oriens-retrohippocampal cell in a later study (Jinno et al., 2007). We assumed trilaminar cells contacted each postsynaptic target with 10 synapses (Table 2), giving a local divergence of 1,544 cells (618 pyramidal cells and 926 interneurons).

3.2 Afferents of the CA1

We used bouton counts and synapse counts from EM studies on the dendrites and somata of CA1 pyramidal cells to quantify their inputs (see Megias et al., 2001; we have reproduced their data with permission in our Table 19). We included the contributions of afferents to the CA1 as well as the local axonal projections of CA1 pyramidal cells and interneurons. In addition, we calculated the convergence of afferents and intrinsic inputs onto a hypothetical average interneuron and compared it to the synapse data available for several neurochemical classes of interneuron (Gulyas et al., 1999; Matyas et al., 2004).

3.2.1 Glutamatergic Afferents of the CA1—

Excitatory inputs arrive mainly from the CA3 (Schaffer Collaterals) and the entorhinal cortex, but also from the nucleus reuniens of the thalamus and other areas (Wouterlood et al., 1990; Sotty et al., 2003; Kajiwara et al., 2008; Klausberger and Somogyi, 2008). Here, we calculated the inputs from the Schaffer Collaterals and entorhinal cortex. The Schaffer Collaterals represent the main excitatory input to the CA1. The entorhinal cortex supplies significantly less excitatory input. There are additional, smaller excitatory inputs as well, though insufficient data exist to quantify them. For example, the subiculum is known to target all layers of the CA1 (Kohler, 1985). The amygdalar input to the CA1 is also excitatory (Klausberger and Somogyi, 2008). There are

also some connections from the subiculum, presubiculum, and parasubiculum as reviewed in Van Strien et al. (2009). In addition, there is glutamatergic input from the septum (Sotty et al., 2003).

It should be noted that the count of non-GABAergic synapses received by the pyramidal cell includes synapses that are not glutamatergic (Megias et al., 2001). Some non-GABAergic synapses are contributed by the cholinergic pathway from the septum. Less commonly, the serotonergic pathway may innervate sparsely the pyramidal cells, though it appears to rely mostly on volume transmission to pyramidal cells (Gulyas et al., 1990; Borhegyi et al., 2004).

Schaffer Collaterals: The CA3 is estimated to contain 230,000 neurons, within the range for 30 day old Wistar rats (210,000 − 250,000, from West et al., 1991). Approximately 11% of neurons in the hippocampus are interneurons (Woodson et al., 1989; also see our Table 2), for a total of 204,700 pyramidal cells and 25,300 interneurons in the CA3.

Though the Schaffer Collaterals innervate both the strata radiatum and oriens of the CA1, there is a gradient in innervation where the CA3c neurons prefer the stratum radiatum and the CA3a neurons prefer the stratum oriens (Amaral and Witter, 1989). The CA3c neurons also tend to synapse more temporally whereas the CA3a neurons synapse more septally (Amaral and Witter, 1989). Therefore, we averaged data from a CA3c and a CA3a neuron to calculate the average input from a CA3 neuron to the CA1. The CA3c pyramidal cell was shown to have about 39,200 boutons within the dorsal area of the ipsilateral hippocampus (Wittner et al., 2007). Approximately 70% of these boutons were found in the CA1 region, so that this single pyramidal cell may contribute 27,440 boutons to the Schaffer Collateral pathway (Wittner et al., 2007). This CA3c neuron was shown to make 94% of its Schaffer Collateral synapses in the stratum radiatum and only 3% in the stratum oriens (Wittner et al., 2007). In contrast, the CA3a neuron was shown to make 64% of its synapses in the stratum oriens, 15% in the stratum pyramidale, and 21% in the stratum radiatum (Sik et al., 1993), for a total of 15,295 boutons. The relative laminar distributions of the Schaffer Collateral boutons yielded the bouton counts per lamina shown in Table 20. We calculated the input of an average CA3 neuron to the Schaffer Collateral pathway, assuming that the bouton distributions for the CA3a and CA3c neurons could be taken as the extreme examples on each end of a uniform gradient (Table 2).

However, this calculated contribution is certainly low. The CA1 pyramidal cell has a total of 28,860 excitatory synapses on its dendrites in the stratum radiatum and oriens (Megias et al., 2001) (see Table 19), which are mainly innervated by the Schaffer Collaterals. This number is much greater than the input calculated from the average of the CA3a and CA3c neurons (Table 20). There are two reasons for the discrepancy. First, the contralateral CA3 axons contribute a significant number of boutons to each CA1 pyramidal cell. Second, at least in the case of the Wittner et al. (2007) axon, the axonal extent of the filled CA3 neuron may have extended outside the slices that contributed to the bouton count, so that the ipsilateral axon fill was incomplete (the axon published in Wittner et al. (2007) was reconstructed from 48 slices 70 um thick in the ipsilateral dorsal hippocampus for a total of 39,200 boutons; earlier work by Li et al. (1994) had estimated a CA3 pyramidal cell could contribute up to 60,000 boutons to the ipsilateral hippocampus). In the case of the Sik et al. (1993) axon fill, the axon was reconstructed from 32 sections 60 um thick of the ipsilateral hippocampus and was said to be a complete reconstruction of the ipsilateral axon. By comparing the total number of available synapses on the CA1 pyramidal cell dendrites in the strata radiatum and oriens with the reported bouton counts from the CA3 pyramidal cells, we estimated that the reported counts represent only 46% of the boutons expected to project to the ipsilateral and contralateral CA1 from each CA3 neuron. The comparison of Schaffer Collateral boutons

per CA1 pyramidal cell and available synapses on the CA1 pyramidal cell (as calculated in Megias et al., 2001) is shown in Table 21. To calculate the boutons available per CA1 pyramidal cell, we multiplied the average CA1-area bouton count by the number of CA3 pyramidal cells, took 93% of the total as synapsing on CA1 pyramidal cells (Takacs et al., 2012), and then divided that total by the number of CA1 pyramidal cells.

We also considered the divergence of the CA3 pyramidal cells within the ipsilateral CA1. For pyramidal cells within the CA3c, most connections made onto CA1 pyramidal cells comprise one to two synapses (Ropireddy and Ascoli, 2011), for an ipsilateral divergence of 12,760 – 25,520 CA1 pyramidal cells. Given the total number of CA1 pyramidal cells, this range corresponded to each CA3c pyramidal cell contacting 4–8% of CA1 pyramidal cells ipsilaterally, in line with the 4–9% potential CA1 pyramidal cell connectivity determined for CA3c pyramidal cells using 3D anatomical reconstruction data (Ropireddy and Ascoli, 2011). The ipsilateral CA1 divergence for the CA3a cell, with its significantly lower bouton count in the CA1, is expected to be much lower. Though no CA3a cells were included in the work of Ropireddy and Ascoli (2011), a CA3b cell was shown to have a much lower connectivity onto the CA1 pyramidal cells (<1%) than the CA3c cells.

Other excitatory afferents: The main source of glutamatergic inputs to the stratum lacunosum-moleculare of the CA1 is the temporoammonic pathway from the entorhinal cortex (Andersen et al., 2007). This pathway is likely responsible for the majority of the excitatory synapses on the distal apical dendrites of CA1 pyramidal cells, though the glutamatergic inputs from the nucleus reuniens in the thalamus also make up a significant portion of synapses (Wouterlood et al., 1990). The input from the nucleus reuniens is differentiated by the presence of VGLUT2 in the boutons (Halasy et al., 2004). The VGLUT2+ boutons are only found in the stratum lacunosum-moleculare (Halasy et al., 2004). We do not know the relative proportion of inputs from the entorhinal cortex versus the nucleus reuniens, so we have assumed that the entorhinal cortex supplies most of the excitatory inputs (Table 2). Together, they contribute about 1,742 synapses, which is the number of distal apical synapses found on a pyramidal cell (Megias et al., 2001) after subtracting a small contribution of the Schaffer Collaterals to the stratum lacunosum-moleculare (see contribution from a CA3c cell, Table 20).

Both the medial and lateral entorhinal cortex project to the CA1, though the lateral projection appears to be stronger (Witter et al., 1988). The number of principal neurons in the entorhinal cortex layer III was found to be 250,000, with 130,000 in the medial entorhinal cortex and 120,000 in the lateral entorhinal cortex (Mulders et al., 1997). We made a cursory estimate of the divergence of the entorhinal cortical neurons to the stratum lacunosum-moleculare. We assumed that both medial and lateral parts contributed proportionally to the stratum lacunosum-moleculare-targeting temporoammonic path, and that all 1,742 of the stratum lacunosum-moleculare synapses were innervated by the temporoammonic path (Table 2). With those assumptions, each entorhinal cortical neuron would need to provide an average of 2,171 boutons to the stratum lacunosum-moleculare-targeting part of the temporoammonic path. Given that the nucleus reuniens input may be significant, this calculation of divergence may be overestimated.

The temporoammonic path also includes an alvear targeting component. Although there are no solid quantitative comparative data, the alvear pathway is considered a minor source of entorhinal cortical input compared to the temporoammonic pathway that targets the stratum lacunosum-moleculare directly, so it must contribute significantly fewer than 1,742 synapses to each CA1 pyramidal cell.

3.3 Convergence onto CA1 pyramidal cells

Next, we calculated the convergence of various neuron types onto a CA1 pyramidal cell. We compared the calculated inputs with the observed synapses on CA1 pyramidal cell dendrites and somata (see Table 19, which reproduces data from Megias et al., 2001).

3.3.1 Excitatory Synapses—Given the calculations above, we estimated that each pyramidal cell received 13,059 – 28,697 synapses from the Schaffer Collateral pathway. Additionally, each pyramidal cell received up to 1,742 synapses from the entorhinal cortex via the stratum lacunosum-moleculare-targeting portion of the temporoammonic pathway, and a smaller number of synapses from the entorhinal cortex via the alvear pathway. Previously, we had calculated that each pyramidal cell receives 197 synapses from other local collaterals. In total, a CA1 pyramidal cell receives approximately 30,636 excitatory inputs (Megias et al., 2001). A summary of the excitatory convergence onto pyramidal cells is given in Table 22.

3.3.2 Perisomatic GABA+ Synapses—Basket cells are known to synapse on and around the pyramidal cell soma, with CCK+ cell synapses being found further out from the soma than PV+ basket cell synapses (Foldy et al., 2010, in mouse). There are approximately 92 synapses, all GABAergic, on the pyramidal cell body; including the proximal oriens and thick radiatum dendrites that extend up to 100 μm from the soma, there are 518 perisomatic, GABAergic synapses (Megias et al., 2001). The ratio of PV:CCK basket cell synapses on the soma is about 2:1 (Foldy et al., 2010, in mouse). We multiplied the number of each type of basket cell by the number of boutons (Table 5) to get the total number of basket cell boutons in the CA1. Then we computed the average number of boutons that can synapse on each pyramidal cell, taking into account their preference for innervating pyramidal cells as discussed earlier. That gave a total of 289 basket cell synapses per pyramidal cell. We assumed that only basket cells synapse on the soma (Table 2). Since only 92 of these 289 synapses are found directly on the soma, we calculated that only 32% of basket cell synapses are on the soma. This calculation is slightly lower than the 51% observed experimentally for basket cells generally (Buhl et al., 1994a), or the 48–77% observed for CCK+ basket cells, specifically (Pawelzik et al., 2002). Subtracting the 92 synapses found on the soma (assuming all somatic GABAergic synapses are made by basket cells, Table 2) gave a total of 197 proximal dendritic synapses made by basket cells. That left 229 of the 518 perisomatic synapses (somatic, proximal basal, and thick, proximal radiatum synapses) unclaimed. However, since other cell types occasionally make perisomatic synapses as well (such as trilaminar cells (Ferraguti et al., 2005), bistratified cells (Buhl et al., 1994a), or ivy cells (Fuentealba et al., 2008a)), those could account for some of the perisomatic synapses found on the pyramidal cell.

To determine the convergence of basket cells onto a pyramidal cell, we divided the total number of synapses contributed from each basket cell type by the average number of synapses per connection made by each basket cell type. Therefore, we calculated that each pyramidal cell is innervated by 17 PV+ basket cells and 13 CCK+ basket cells.

3.3.3 Axon Initial Segment GABA+ Synapses—There are at least 25 synapses on the axon of the CA1 pyramidal cell (Megias et al., 2001). This count only includes proximal synapses, though there are likely more synapses distally (Megias et al., 2001). These axonal synapses were not included in the dendritic or somatic counts for pyramidal cells, given in Table 19. Dividing the total number of boutons from all axo-axonic cells by the total number of pyramidal cells in the CA1, we calculated that there are 34 axo-axonic boutons for each pyramidal cell (assuming they only innervate pyramidal cells, see Buhl et al., 1994a,b) and that a pyramidal cell receives input from about six axo-axonic cells on its proximal axon.

3.3.4 Proximal Dendritic GABA+ Synapses—The number of GABAergic synapses found on the proximal basal and apical dendrites of a pyramidal cell total 953 (Table 19) (Megias et al., 2001). A number of interneuron types synapse on these proximal dendrites of the pyramidal cell, which include the dendrites in the strata oriens and radiatum. This category encompasses bistratified cells, ivy cells, Schaffer Collateral-associated (SCA) cells, apical dendritic innervating (ADI) cells, large calbindin cells, trilaminar cells, and various projection cells (Klausberger and Somogyi, 2008). Note that some of the neurons associated with the stratum lacunosum-moleculare also synapse in the stratum radiatum. For example, neurogliaform cells located close to the strata lacunosum-moleculare/radiatum border make many of their synapses in the stratum radiatum (Vida et al., 1998). For this assessment, we generally assumed that the distally projecting neuron types only make synapses on the distal apical dendrites in the stratum lacunosom-moleculare (Table 2). However, we did account for the subset of neurogliaform cells identified in the stratum radiatum as synapsing within the stratum radiatum (see neuron numbers calculation above) and a small fraction of O-LM cell axons remaining in the stratum oriens.

Bistratified Cell Synapses: Bistratified cells synapse on the small and medium sized dendrites, generally avoiding the main apical dendrite of the pyramidal cell (Klausberger et al., 2004). Multiplying the average number of boutons per bistratified cell by the estimated number of bistratified cells gave an average of 104 boutons per pyramidal cell, assuming that 92% of their boutons innervate pyramidal cells. Given that bistratified cells usually make 10 synapses per connection, each pyramidal cell receives input from 10 bistratified cells. The inputs from the bistratified cells represent about 7.5% of the inhibitory input synapses on the dendrites in strata oriens, pyramidale, and radiatum dendrites of the CA1 pyramidal cell.

Projection Cell Synapses: To calculate the contributions of the double projection and oriens-retrohippocampal cells to CA1 pyramidal cell innervation, we assumed that they had a similar number of local boutons as the so-called back-projection cell (Table 2). We calculated that these projection cells (which make up 4% of interneurons) could supply 2% of the available inhibitory dendritic synapses on CA1 pyramidal cells. The contribution of the other projection cell types could not be calculated since their cell numbers are unknown.

Ivy Cell Synapses: Given the number of ivy cells and the calculation of their classical bouton count, we estimated that a CA1 pyramidal cell receives 422 synapses from ivy cells. Ivy cells therefore innervate 28% of the synapses on the strata radiatum, pyramidale, and oriens dendrites of the pyramidal cell. Since ivy cells make about 10 synapses per connection, each pyramidal cell receives classical synaptic input from 42 ivy cells. If there are ivy cells that only influence pyramidal cells through volume transmission without making any classical synapses, we have not included them in this calculation of convergence.

Stratum Radiatum Neurogliaform Cell Synapses: As neurogliaform cells are often found near the border of the strata radiatum and lacunosum-moleculare, their axons sometimes fall within the stratum radiatum. Here, we made the simplifying assumption that those neurogliaform cells found in the stratum radiatum contribute their boutons to dendrites in the stratum radiatum. Earlier we had calculated that there were 610 neurogliaform cells in the stratum radiatum; therefore, they are expected to contribute a total of 24 boutons to the stratum radiatum dendrites of each CA1 pyramidal cell. Since neurogliaform cells make 10 synapses per connection, a single CA1 pyramidal cell likely receives classical synaptic input from two neurogliaform cells in the stratum radiatum. As with the ivy cells, if some

neurogliaform cells contact pyramidal cells only through volume transmission but not classical synapses, they were not included in this calculation.

Schaffer Collateral Associated Cell Synapses: SCA cells synapse mainly in the stratum radiatum, but also in the stratum oriens. In the stratum radiatum, SCA cells prefer to synapse on the oblique dendrites rather than the main shaft (Klausberger, 2009). We estimated that a CA1 pyramidal cell receives 14 synapses from SCA cells. Since SCA cells make about six synapses per connection, each pyramidal cell receives input from about two SCA cells.

Apical Dendritic Innervating Cell Synapses: ADI cells have similar targets to SCAs but tend to innervate the main shaft more than SCA cells; in general, they prefer the large apical dendrites (Klausberger et al., 2005; Klausberger, 2009). We do not know much about the axonal length or bouton density of ADI cells. We estimated above that there are 390 ADI cells in the CA1, but without any bouton data, their convergence cannot be estimated.

Other Proximal Dendritic Synapses: Several other neurons known to innervate the basal and proximal apical dendrites have not been included here, such as so-called back projection, trilaminar, RADI, large calbindin, and some lesser-known CCK+ cell types. The numbers of these neurons are not known very precisely, nor are their bouton counts, with the exception of the bouton counts for the trilaminar cells.

Assessing the difference between interneuron boutons available for synapsing onto pyramidal cells and GABAergic synapses on pyramidal cell dendrites, we find that there are still available synapses on the dendrites for which we have not determined the source. In the stratum oriens, 290 inhibitory synapses on the basal dendrites (128 of them perisomatic) were still unclaimed. In the stratum radiatum, there were still 333 inhibitory synapses (87 perisomatic) remaining.

3.3.5 Distal Dendritic GABA+ Synapses—Neurogliaform, O-LM, and lesser well-known types such as the perforant path associated (PPA) and radiatum-retrohippocampal projection cells are known to synapse on the distal dendrites in the stratum lacunosum-moleculare (Klausberger and Somogyi, 2008). The total number of synapses made onto the distal apical dendrites of a pyramidal cell is 335 (Megias et al., 2001).

Neurogliaform Cell Synapses: As discussed above, a large portion of neurogliaform cell boutons are found in the stratum lacunosum-moleculare. We made the simplifying assumption that all of the neurogliaform cells found in the stratum lacunosum-moleculare contributed their boutons to that layer. Therefore, 2,970 neurogliaform cells in the stratum lacunosum-moleculare contribute an average of 116 classical boutons per pyramidal cell and innervate 35% of stratum lacunosum-moleculare inhibitory synapses. It follows that each pyramidal cell receives input from 12 neurogliaform cells in the stratum lacunosum-moleculare and 14 neurogliaform cells overall, given that neurogliaform cells have been observed to make 10 synapses per connection (Tamas et al., 2003; also, see Table 2). As mentioned above, if some neurogliaform cells contact pyramidal cells only through volume transmission but not classical synapses, they were not included in this calculation.

O-LM Cell Synapses: About 99% of O-LM boutons remained in the CA1 (Sik et al., 1995), giving a total of 77 synapses per pyramidal cell (72 on the distal apical dendrites and 5 on the basal dendrites). We estimated that O-LM cells make 10 synapses per connection (Table 2) based on light microscopic observations (Maccaferri et al., 2000), such that eight O-LM cells converge on a single pyramidal cell.

PPA Cell Synapses: PPA cells seem to innervate small to medium sized dendrites mostly in the stratum lacunosum-moleculare (Vida et al., 1998; Klausberger, 2009). Accounting for the estimated number of PPA cells (490) and the local bouton count (8,000), the average number of boutons available per pyramidal cell is 12. Given that PPA cells make about six synapses per connection, we calculated a convergence of two PPA cells onto each pyramidal cell.

Other Distal Dendritic Synapses: An average of 99 distal, stratum lacunosum-moleculare dendritic synapses per pyramidal cell remain unclaimed. Some of these synapses may be innervated by the radiatum-retrohippocampal cell, but we have no bouton information for that cell so we cannot calculate its contribution.

3.3.6 Summary of inhibitory convergence onto pyramidal cells—Table 23 summarizes the estimated convergence of interneurons onto a single CA1 pyramidal cell, while Table 24 gives laminar innervation calculations. Although a CA1 pyramidal cell has been shown to have about 1,840 inhibitory synapses on its dendrites, soma, and axon, we only calculated 1,118 inhibitory inputs. Therefore, 39% of the inhibitory inputs remain unspecified by our calculations. There are several possible reasons for this discrepancy. We should consider that axonal fills of interneurons may be incomplete, or bouton density may be higher, or the fraction of boutons that participate in classical synapses from neurogliaform family neurons may be much higher, or the fraction of CA1 neurons that are interneurons may be higher than previously reported. Though some afferent projections to the CA1 are GABAergic, they mainly target interneurons rather than pyramidal cells (Freund and Antal, 1988; Gulyas et al., 1990; Melzer et al., 2012, in mouse), so we do not consider them significant here.

3.4 Convergence onto CA1 interneurons

Here, we first summarized available data about synapses onto various interneuron classes. Then we looked for a way to compare the number of input synapses with the number of boutons available to innervate them. Unfortunately, there are not sufficient data available to calculate the inputs for individual interneuron subtypes. Instead, we calculated the convergence onto a hypothetical average interneuron. This concept should not be taken to represent any particular interneuron type in the CA1; because the interneurons are so diverse, no average could adequately describe them (Soltesz, 2006). However, we believe the concept of a hypothetical average interneuron is helpful in this assessment for comparing available boutons with available input synapses.

For some neurochemical classes of interneuron, the input synapse numbers have been calculated (Table 25). These classes include CCK+, PV+, CB+, and CR+ cells. The CCK+ cell class represents CCK+ basket cells only. The PV+ class was heterogeneous, but the morphological traits varied smoothly such that there were no distinctive groups (Gulyas et al., 1999); it is likely that multiple PV+ cell types are included. The identity of the CB+ cell class was unclear. Judging from their dendritic distribution, the Type 1 neurons (Gulyas et al., 1999) could be large calbindin cells or perhaps CB+ bistratified cells. Since they do not have many dendrites in the stratum lacunosum-moleculare, they seem less likely to be SCA or PPA cells. The Type 2 neurons mentioned here but not analyzed look to be double projection cells (Gulyas et al., 1999). The CR+ cell type is likely to include multiple interneuron-specific cell types (Gulyas et al., 1999).

3.4.1 Excitatory afferents—Takacs et al. (2012) found that 93% of Schaffer Collateral synapses were made onto pyramidal cells, while 7% of synapses were made onto interneurons. We started with the number of Schaffer Collateral synapses on pyramidal cells

and used the ratio to determine the Schaffer Collateral synapses available for interneurons. This gave an average of 7,952–17,476 Schaffer Collateral synapses onto each interneuron (Table 26), depending on whether we counted only the observed boutons on the CA3 neurons or what we calculated must be the total number based on the available CA1 pyramidal cell synapses in the strata radiatum and oriens.

Performing the same exercise with the remaining stratum lacunosum-moleculare inputs (assuming they are all from the entorhinal cortex, Table 2) gave an additional 1,394 entorhinal cortical boutons available per interneuron, since 9% of the entorhinal cortical input to the stratum lacunosum-moleculare synapses on interneurons (Takacs et al., 2012). Additionally, there are 2,211 boutons per interneuron from the local collaterals of the CA1. This gave a total of 11,557–21,081 excitatory inputs (Table 26), much higher than most of the observed values in those classes reported in Table 6, where the weighted average gives 9,461 excitatory inputs per interneuron. Note that it does not include entorhinal cortical inputs coming from the alvear pathway (in which the fraction of synapses made onto interneurons is high, at 21%, see Takacs et al., 2012), so the actual number of available excitatory boutons may be even higher. Additionally, interneurons receive non-GABAergic input from subcortical sources. They also receive some cholinergic input from the septum, and serotonergic and glutamatergic input from the raphe (Gulyas et al., 1990; Freund et al., 1990; Freund and Gulyas, 1997; Varga et al., 2009). Of course, not all interneurons receive inputs from all excitatory sources, so there may be a significant variation in total number of excitatory inputs across all interneuron types.

3.4.2 Inhibitory inputs—There is not sufficient quantitative information to calculate the convergence of inhibitory inputs onto specific interneuron types. However, an excellent recent qualitative review of interneuron-interneuron connectivity is given in Chamberland and Topolnik (2012) and a detailed analysis of specific connections seen in the literature is underway as part of the Hippocampome project (hippocampome.org). Instead, we employ the concept of the hypothetical average interneuron, as described above. Table 27 calculates the number of local GABAergic boutons received by the hypothetical average interneuron. The average number of local boutons, 692, is reasonable given the number of GABAergic inputs (local and projections) received by several classes of interneurons (462 – 3,080 with a weighted average of 1,274, see Table 6). Since the estimate does not include the contributions from the interneuron-specific cells or inhibitory afferents, the actual number would be higher. Regarding the afferents, note that interneurons also receive GABAergic input from the entorhinal cortex and the septum (Freund and Antal, 1988; Borhegyi et al., 2004; Melzer et al., 2012, in mouse). Finally, when considering the difference between the hypothetical average interneuron and a real interneuron class, it should be realized that the laminar distribution of interneuron dendrites is highly variable. Therefore, some interneurons receive no input from a particular interneuron type. Conversely, those interneurons that do receive input from a particular interneuron type may receive significantly more input than would the hypothetical average interneuron.

4 Discussion

We were able to confidently estimate the numbers of the most abundant interneuron types in the CA1, including the PV+ basket, bistratified and axo-axonic cells, the O-LM cells, the CCK+ basket cells, and the neurogliaform family cells (ivy and neurogliaform). Together, these cell types constituted 70% of GABAergic interneurons in the CA1. We also estimated that interneuron-specific cells make up an additional 19% of GABAergic interneurons. By making some layer-based assumptions, we were able to estimate the numbers of an additional 5% of interneurons comprising the remaining CCK+ cell types. The remaining SOM+ cells and other projections cells were less readily quantifiable, but appeared to

constitute 5−7% of the GABAergic interneurons, with other, more obscure cell types making up the remaining fraction (about 1%).

Regarding the calculations of cell numbers, some previous estimates exist. Freund and Gulyas (1997) estimated that CR+ cells comprise 13% of all hippocampal interneurons. By our calculations (adding IS I, IS III and possibly the small subset of CB- septally projecting cells), the CR+ cells constitute 14–15% of CA1 cells, roughly the same as the previous estimate. Baude et al. (2007) estimated the fraction of interneurons that were PV+ basket, bistratified, or axo-axonic cells as 12%, 5%, and 3%, respectively. We reached a similar conclusion, with fractions of 14%, 6%, and 4%, for PV+ basket, bistratified, and axo-axonic cells.

Jinno and Kosaka (2006) have provided experimental observations of the neurochemical composition per layer and laminar distribution, but for mouse hippocampus. It is not clear whether these data in rat and mouse should match, as the laminar distribution data for various markers have been shown to be somewhat different for rat (Kosaka et al., 1985; Kosaka et al., 1987; Kosaka et al., 1988; Nomura et al., 1997b; Pawelzik et al., 2002; Fuentealba et al., 2010) and mouse (Jinno and Kosaka, 2006), as seen in Tables 10, 11, 14, and 17. As more data about the expression of all markers by each interneuron type become available and standardized (hippocampome.org), it will be possible to calculate the expected neurochemical composition per layer in rat, based on the cell number estimates provided here.

In quantitatively assessing the CA1, we have taken most of our data from the rat. However, some data were not available for the rat CA1 and so we used observations made in mouse, instead. This includes the percent of SOM+ cells projecting to the medial septum. In addition, the ratio of PV+ basket cell boutons to CCK+ basket cell boutons, used to calculate the total number of CCK+ basket cells, was averaged from two experiments done in mouse. Finally, the number of synapses per connection made by PV+ basket cells and CCK+ basket cells onto pyramidal cells was taken from mouse data. We are not aware of published differences between rat and mouse regarding the projection cells or the basket cell connectivity.

For a few data points, we relied on data from other parts of the brain than the CA1. This occurred for the neurogliaform family bouton properties: the fraction of boutons forming classical synapses (taken from somatosensory cortex) and the density of boutons (taken from the dentate gyrus and CA3). We are not aware of significant differences between neurogliaform cells of the somatosensory cortex and the CA1. However, we have taken care to note the fraction of boutons forming classical synapses in the assumption table. Because the bouton densities in the dentate gyrus and CA3 were similar, we believe that the bouton densities of neurogliaform family cells in the CA1 will also be similar to the those in the dentate gyrus and CA3.

In estimating the connectivity of the CA1, we performed an initial calculation of the excitatory and inhibitory convergence onto CA1 pyramidal cells, as well as onto a hypothetical average interneuron. The calculation revealed that we could only account for about half of the excitatory and inhibitory inputs to CA1 pyramidal cells based on known afferent and interneuron axon data and our calculated cell numbers. We were surprised by the magnitude of the difference and hope that the exposure of this difference will drive more experiments to fill in this gap of our knowledge. In contrast to the pyramidal cell, the convergence onto the hypothetical average interneuron aligned with or exceeded our expectations based on the observed input synapses for several classes of interneurons.

In general, we expect that our estimates could be refined as the projection cell types become better defined and their marker combinations further characterized. In addition, more sophisticated ways are needed to distinguish the various CCK+ cell types, rather than relying on laminar position. We also look forward to more data becoming available for the lesser-known cell types, such as the large calbindin cell, RADI cell, and the enkephalin-expressing subicular projecting cell.

More in vivo axon fills of interneurons would help refine the divergence calculations for axo-axonic cells, CCK+ cells, and interneuron-specific cells. Also, convergence data in the form of what percent of inhibitory inputs onto pyramidal cells are associated with the various neurochemical markers would provide a validation of our convergence calculations and could explain the source of the remaining 39% of GABAergic inputs that were unknown in this assessment. Further quantification of excitatory inputs is also necessary, especially those targeting the stratum lacunosum-moleculare. With the current, quantitative knowledge of the CA1, researchers will be better able to hypothesize about and quantify the roles of the various interneuron types in network functions. In addition, the knowledge base will also be critically important for the construction of more accurate, biologically constrained computer models of the CA1, similar to the data-driven models of the dentate gyrus (Santhakumar et al., 2005; Morgan and Soltesz, 2008; Schneider et al., 2012). The assembled data will also allow better contrasting of the network makeup of the CA3 and other regions with that of the CA1.

We propose that additional anatomical experiments be carried out to validate our quantifications, to replace the assumptions made in Table 2 with experimental data, and to fully determine the convergence of each interneuron type onto pyramidal cells and interneurons. It seems appropriate to suggest that the rat CA1 region can and should be fully quantified in the near future. When such a milestone is reached, the assessment can be further extended by comparison among species, strains, or individuals. This “Big Data” approach (Mayer-Schonberger and Cukier, 2013) to neuroanatomy will enable researchers to quantify fully the role of each interneuron within the CA1 network and to assess precisely the anatomical bases of the differences in network function across species.

Acknowledgments

We thank our anonymous reviewers, as well as Laszlo Acsady, Marco Capogna, Tamas Freund, Attila Gulyas, Norbert Hajos, Istvan Katona, Thomas Klausberger, Esther Krook-Magnuson, Karri Lamsa, Sang-hun Lee, Peter Somogyi, and Csaba Varga for helpful comments on this manuscript. This work was supported by the National Science Foundation under Grant No. DGE-0808392 (M.B.) and by the National Institutes of Health under Grant No. NS35915 (I.S.).

Grants:

Grant sponsor: National Institutes of Health; Grant number: NS35915

Grant sponsor: National Science Foundation; Grant number: DGE-0808392

References

Acsady L, Arabadzisz D, Freund T. Correlated morphological and neurochemical features identify different subsets of vasoactive intestinal polypeptide-immunoreactive interneurons in rat hippocampus. Neuroscience. 1996a; 73:299–315. [PubMed: 8783251]

Acsady L, Gorcs T, Freund T. Different populations of vasoactive intestinal polypeptide-immunoreactive interneurons are specialized to control pyramidal cells or interneurons in the hippocampus. Neuroscience. 1996b; 73:317–334. [PubMed: 8783252]

Aika Y, Ren J, Kosaka K, Kosaka T. Quantitative analysis of GABA-like-immunoreactive and parvalbumin-containing neurons in the CA1 region of the rat hippocampus using a stereological method, the disector. Exp Brain Res. 1994; 99:267–276. [PubMed: 7925807]

Ali AB, Deuchars J, Pawelzik H, Thomson AM. CA1 pyramidal to basket and bistratified cell EPSPs: dual intracellular recordings in rat hippocampal slices. J Physiol. 1998; 507:201–217. [PubMed: 9490840]

Amaral D, Witter M. The three-dimensional organization of the hippocampal formation: a review of anatomical data. Neuroscience. 1989; 31:571–591. [PubMed: 2687721]

Andersen, P.; Morris, R.; Amaral, D.; Bliss, T.; O'Keefe, J. The Hippocampus Book. New York: Oxford University Press; 2007. p. 872

Armstrong C, Krook-Magnuson E, Soltesz I. Neurogliaform and ivy cells: a major family of nNOS expressing GABAergic neurons. Front Neural Circ. 2012; 6:23.

Armstrong C, Szabadics J, Tamas G, Soltesz I. Neurogliaform cells in the molecular layer of the dentate gyrus as feed-forward γ-aminobutyric acidergic modulators of entorhinal-hippocampal interplay. J Comp Neurol. 2011; 519:1476–1491. [PubMed: 21452204]

Ascoli G, Alonso-Nanclares L, Anderson S, Barrionuevo G, Benavides-Piccione R, Burkhalter A, Buzsaki G, Cauli B, Defelipe J, Fairen A, et al. Petilla terminology: nomenclature of features of GABAergic interneurons of the cerebral cortex. Nat Rev Neurosci. 2008; 9:557–568. [PubMed: 18568015]

Baude A, Bleasdale C, Dalezios Y, Somogyi P, Klausberger T. Immunoreactivity for the GABAA receptor α1 subunit, somatostatin and connexin36 distinguishes axo-axonic, basket, and bistratified interneurons of the rat hippocampus. Cereb Cortex. 2007; 17:2094–2107. [PubMed: 17122364]

Biro A, Holderith N, Nusser Z. Quantal size is independent of the release probability at hippocampal excitatory synapses. J Neurosci. 2005; 25:223–232. [PubMed: 15634785]

Borhegyi Z, Varga V, Szilagyi N, Fabo D, Freund T. Phase segregation of medial septal GABAergic neurons during hippocampal theta activity. J Neurosci. 2004; 24:8470–8479. [PubMed: 15456820]

Buhl E, Cobb S, Halasy K, Somogyi P. Properties of unitary IPSPs evoked by anatomically identified basket cells in the rat hippocampus. Eur J Neurosci. 1995; 7:1989–2004. [PubMed: 8528474]

Buhl E, Halasy K, Somogyi P. Diverse sources of hippocampal unitary inhibitory postsynaptic potentials and the number of synaptic release sites. Nature. 1994a; 368:823–828. [PubMed: 8159242]

Buhl E, Han Z, Lorinczi Z, Stezhka V, Karnup S, Somogyi P. Physiological properties of anatomically identified axo-axonic cells in the rat hippocampus. J Neurophysiol. 1994b; 71:1289–1307. [PubMed: 8035215]

Chamberland S, Topolnik L. Inhibitory control of hippocampal inhibitory neurons. Front Neurosci. 2012; 6:165. [PubMed: 23162426]

Chen K, Ratzliff A, Hilgenberg L, Gulyas A, Freund T, Smith M, Dinh T, Piomelli D, Mackie K, Soltesz I. Long-term plasticity of endocannabinoid signaling induced by developmental febrile seizures. Neuron. 2003; 39:599–611. [PubMed: 12925275]

Cobb S, Halasy K, Vida I, Nyiri G, Tamas G, Buhl E, Somogyi P. Synaptic effects of identified interneurons innervating both interneurons and pyramidal cells in the rat hippocampus. Neuroscience. 1997; 79:629–648. [PubMed: 9219929]

Cope D, Maccaferri G, Marton L, Roberts J, Cobden P, Somogyi P. Cholecystokinin-immunopositive basket and Schaffer collateral-associated interneurons target different domains of pyramidal cells in the CA1 area of the rat hippocampus. Neuroscience. 2002; 109:63–80. [PubMed: 11784700]

Deuchars J, Thomson A. CA1 pyramid-pyramid connections in rat hippocampus in vitro: dual intracellular recordings with biocytin filling. Neuroscience. 1996; 74:1009–1018. [PubMed: 8895869]

Elfant D, Pal B, Emptage N, Capogna M. Specific inhibitory synapses shift the balance from feedforward to feedback inhibition of hippocampal CA1 pyramidal cells. Eur J Neurosci. 2008; 27:104–113. [PubMed: 18184315]

Esclapez M, Hirsch JC, Ben-Ari Y, Bernard C. Newly formed excitatory pathways provide a substrate for hyperexcitability in experimental temporal lobe epilepsy. J Comp Neurol. 1999; 408:449–460. [PubMed: 10340497]

Ferraguti F, Cobden P, Pollard M, Cope D, Shigemoto R, Watanabe M, Somogyi P. Immunolocalization of metabotropic glutamate receptor 1α (mGluR1α) in distinct classes of interneuron in the CA1 region of the rat hippocampus. Hippocampus. 2004; 14:193–215. [PubMed: 15098725]

Ferraguti F, Klausberger T, Cobden P, Baude A, Roberts J, Szucs P, Kinoshita A, Shigemoto R, Somogyi P, Dalezios Y. Metabotropic glutamate receptor 8-expressing nerve terminals target subsets of GABAergic neurons in the hippocampus. J Neurosci. 2005; 25:10520–10536. [PubMed: 16280590]

Foldy C, Lee SH, Morgan RJ, Soltesz I. Regulation of fast-spiking basket cell synapses by the chloride channel ClC-2. Nat Neurosci. 2010; 13:1047–1049. [PubMed: 20676104]

Freund T, Antal M. GABA-containing neurons in the septum control inhibitory interneurons in the hippocampus. Nature. 1988; 336:170–173. [PubMed: 3185735]

Freund T, Buzsaki G. Interneurons of the hippocampus. Hippocampus. 1996; 6:347–470. [PubMed: 8915675]

Freund T, Gulyas A. Inhibitory control of GABAergic interneurons in the hippocampus. Can J Physiol Pharmacol. 1997; 75:479–487. [PubMed: 9250381]

Freund T, Gulyas A, Acsady L, Gorcs T, Toth K. Serotonergic control of the hippocampus via local inhibitory interneurons. Proc Natl Acad Sci U S A. 1990; 87:8501–8505. [PubMed: 1700433]

Fuentealba P, Begum R, Capogna M, Jinno S, Marton L, Csicsvari J, Thomson A, Somogyi P, Klausberger T. Ivy cells: a population of nitric-oxide-producing, slow-spiking GABAergic neurons and their involvement in hippocampal network activity. Neuron. 2008a; 57:917–929. [PubMed: 18367092]

Fuentealba P, Tomioka R, Dalezios Y, Marton L, Studer M, Rockland K, Klausberger T, Somogyi P. Rhythmically active enkephalin-expressing GABAergic cells in the CA1 area of the hippocampus project to the subiculum and preferentially innervate interneurons. J Neurosci. 2008b; 28:10017–10022. [PubMed: 18829959]

Fuentealba P, Klausberger T, Karayannis T, Suen WY, Huck J, Tomioka R, Rockland K, Capogna M, Studer M, Morales M, Somogyi P. Expression of COUP-TFII nuclear receptor in restricted GABAergic neuronal populations in the adult rat hippocampus. J Neurosci. 2010; 30:1595–1609. [PubMed: 20130170]

Graves A, Moore S, Bloss E, Mensh B, Kath W, Spruston N. Hippocampal pyramidal neurons comprise two distinct cell types that are countermodulated by metabotropic receptors. Neuron. 2012; 76:776–789. [PubMed: 23177962]

Gulyas AI, Hajos N, Katona I, Freund T. Interneurons are the local targets of hippocampal inhibitory cells which project to the medial septum. Eur J Neurosci. 2003; 17:1861–1872. [PubMed: 12752786]

Gulyas AI, Toth K, Danos P, Freund T. Subpopulations of GABAergic neurons containing parvalbumin, calbindin D28k, and cholecystokinin in the rat hippocampus. J Comp Neurol. 1991; 312:371–378. [PubMed: 1721075]

Gulyas A, Gorcs T, Freund T. Innervation of different peptidecontaining neurons in the hippocampus by GABAergic septal afferents. Neuroscience. 1990; 37:31–44. [PubMed: 1978740]

Gulyas A, Hajos N, Freund T. Interneurons containing calretinin are specialized to control other interneurons in the rat hippocampus. J Neurosci. 1996; 16:3397–3411. [PubMed: 8627375]

Gulyas A, Miles R, Sik A, Toth K, Tamamaki N, Freund T. Hippocampal pyramidal cells excite inhibitory neurons through a single release site. Nature. 1993; 366:683–687. [PubMed: 8259211]

Gulyas A, Toth K, McBain C, Freund T. Stratum radiatum giant cells: a type of principal cell in the rat hippocampus. Eur J Neurosci. 2001; 10:3813–3822. [PubMed: 9875359]

Gulyas AI, Megias M, Emri Z, Freund TF. Total number and ratio of excitatory and inhibitory synapses converging onto single interneurons of different types in the CA1 area of the rat hippocampus. J Neurosci. 1999; 19:10082–10097. [PubMed: 10559416]

Hajos N, Mody I. Synaptic communication among hippocampal interneurons: Properties of spontaneous IPSCs in morphologically identified cells. J Neurosci. 1997; 17:8427–8442. [PubMed: 9334415]

Halasy K, Hajszan T, Kovacs E, Lam T, Leranth C. Distribution and origin of vesicular glutamate transporter 2-immunoreactive fibers in the rat hippocampus. Hippocampus. 2004; 14:908–918. [PubMed: 15382259]

Halasy K, Buhl EH, Lorinczi Z, Tamas G, Somogyi P. Synaptic target selectivity and input of GABAergic basket and bistratified interneurons in the CA1 area of the rat hippocampus. Hippocampus. 1996; 6:306–329. [PubMed: 8841829]

Jinno S. Structural organization of long-range GABAergic projection system of the hippocampus. Front Neuroanat. 2009; 3:1–9. [PubMed: 19169410]

Jinno S, Kosaka T. Cellular architecture of the mouse hippocampus: a quantitative aspect of chemically defined GABAergic neurons with stereology. Neurosci Res. 2006; 56:229–245. [PubMed: 16930755]

Jinno S, Klausberger T, Marton LF, Dalezios Y, Roberts JDB, Fuentealba P, Bushong EA, Henze D, Buzsaki G, Somogyi P. Neuronal diversity in GABAergic long-range projections from the hippocampus. J Neurosci. 2007; 27:8790–8804. [PubMed: 17699661]

Kajiwara R, Wouterlood F, Sah A, Boekel A, te Bulte LB, Witter M. Convergence of entorhinal and CA3 inputs onto pyramidal neurons and interneurons in hippocampal area CA1 - an anatomical study in the rat. Hippocampus. 2008; 18:266–280. [PubMed: 18000818]

Katona I, Acsády L, Freund T. Postsynaptic targets of somatostatin-immunoreactive interneurons in the rat hippocampus. Neuroscience. 1999a; 88:37–55. [PubMed: 10051188]

Katona I, Sperlagh B, Sik A, Kafalvi A, Vizi ES, Mackie K, Freund TF. Presynaptically located CB1 cannabinoid receptors regulate GABA release from axon terminals of specific hippocampal interneurons. J Neurosci. 1999b; 19:4544–4558. [PubMed: 10341254]

Klausberger T. GABAergic interneurons targeting dendrites of pyramidal cells in the CA1 area of the hippocampus. Eur J Neurosci. 2009; 30:947–957. [PubMed: 19735288]

Klausberger T, Marton L, O'Neill J, Huck J, Dalezios Y, Fuentealba P, Suen WY, Papp E, Kaneko T, Watanabe M, Csicsvari J, Somogyi P. Complementary roles of cholecystokinin- and parvalbumin-expressing GABAergic neurons in hippocampal network oscillations. J Neurosci. 2005; 25:9782–9793. [PubMed: 16237182]

Klausberger T, Marton LF, Baude A, Roberts JD, Magill PJ, Somogyi P. Spike timing of dendrite-targeting bistratified cells during hippocampal network oscillations in vivo. Nat Neurosci. 2004; 7:41–47. [PubMed: 14634650]

Klausberger T, Somogyi P. Neuronal diversity and temporal dynamics: the unity of hippocampal circuit operations. Science. 2008; 321:53–57. [PubMed: 18599766]

Kohler C. Intrinsic projections of the retrohippocampal region in the rat brainIThe subicular complex. J Comp Neurol. 1985; 236:504–522. [PubMed: 3902916]

Kosaka T, Katsumaru H, Hama K, Wu JY, Heizmann C. GABAergic neurons containing the Ca2+-binding protein parvalbumin in the rat hippocampus and dentate gyrus. Brain Res. 1987; 419:119–130. [PubMed: 3315112]

Kosaka T, Kosaka K, Tateishi K, Hamaoka Y, Yanaihara N, Wu JY, Hama K. GABAergic neurons containing CCK-8-like and/or VIP-like immunoreactivities in the rat hippocampus and dentate gyrus. J Comp Neurol. 1985; 239:420–430. [PubMed: 2413092]

Kosaka T, Wu JY, Benoit R. GABAergic neurons containing somatostatin-like immunoreactivity in the rat hippocampus and dentate gyrus. Exp Brain Res. 1988; 71:388–398. [PubMed: 3169171]

Lee SH, Foldy C, Soltesz I. Distinct endocannabinoid control of GABA release at perisomatic and dendritic synapses in the hippocampus. J Neurosci. 2010; 30:7993–8000. [PubMed: 20534847]

Li XG, Somogyi P, Tepper J, Buzsaki G. Axonal and dendritic arborization of an intracellularly labeled chandelier cell in the CA1 region of rat hippocampus. Exp Brain Res. 1992; 90:519–525. [PubMed: 1385200]

Li XG, Somogyi P, Ylinen A, Buzsaki G. The hippocampal CA3 network: an in vivo intracellular labeling study. J Comp Neurol. 1994; 339:181–208. [PubMed: 8300905]

Maccaferri G, David J, Roberts B, Szucs P, Cottingham C, Somogyi P. Cell surface domain specific postsynaptic currents evoked by identified GABAergic neurones in rat hippocampus in vitro. J Physiol. 2000; 524:91–116. [PubMed: 10747186]

Maccaferri G. Stratum oriens horizontal interneurone diversity and hippocampal network dynamics. J Physiol. 2005; 562:73–80. [PubMed: 15498801]

Matyas F, Freund TF, Gulyas AI. Convergence of excitatory and inhibitory inputs onto CCK-containing basket cells in the CA1 area of the rat hippocampus. Eur J Neurosci. 2004; 19:1243–1256. [PubMed: 15016082]

Mayer-Schonberger, V.; Cukier, K. Big Data: A Revolution That Will Transform How We Live, Work, and Think. New York: Houghton Mifflin Harcourt Publishing Company; 2013. p. 256

Megias M, Emri Z, Freund T, Gulyas A. Total number and distribution of inhibitory and excitatory synapses on hippocampal CA1 pyramidal cells. Neuroscience. 2001; 102:527–540. [PubMed: 11226691]

Melzer S, Michael M, Caputi A, Eliava M, Fuchs E, Whittington M, Monyer H. Long-range-projecting GABAergic neurons modulate inhibition in hippocampus and entorhinal cortex. Science. 2012; 335:1506–1510. [PubMed: 22442486]

Miles R, Toth K, Gulyas AI, Hajos N, Freund TF. Differences between somatic and dendritic inhibition in the hippocampus. Neuron. 1996; 16:815–823. [PubMed: 8607999]

Miyashita T, Rockland KS. GABAergic projections from the hippocampus to the retrosplenial cortex in the rat. Eur J Neurosci. 2007; 26:1193–1204. [PubMed: 17767498]

Mizuseki K, Diba K, Pastalkova E, Buzsaki G. Hippocampal CA1 pyramidal cells form functionally distinct sublayers. Nat Neurosci. 2011; 14:1174–1181. [PubMed: 21822270]

Morgan R, Soltesz I. Nonrandom connectivity of the epileptic dentate gyrus predicts a major role for neuronal hubs in seizures. Proc Nat Acad Sci U S A. 2008; 105:6179–6184.

Mulders W, West M, Slomianka L. Neuron numbers in the presubiculum, parasubiculum, and entorhinal area of the rat. J Comp Neurol. 1997; 385:83–94. [PubMed: 9268118]

Nomura T, Fukuda T, Aika Y, Heizmann C, Emson P, Kobayashi T, Kosaka T. Distribution of nonprincipal neurons in the rat hippocampus, with special reference to their dorsoventral difference. Brain Res. 1997a; 751:64–80. [PubMed: 9098569]

Nomura T, Fukuda T, Aika Y, Heizmann C, Emson P, Kobayashi T, Kosaka T. Laminar distribution of non-principal neurons in the rat hippocampus, with special reference to their compositional difference among layers. Brain Res. 1997b; 764:197–204. [PubMed: 9295210]

Olah S, Fule M, Komlosi G, Varga C, Baldi R, Barzo P, Tamas G. Regulation of cortical microcircuits by unitary GABA-mediated volume transmission. Nature. 2009; 461:1278–1281. [PubMed: 19865171]

Parra P, Gulyas A, Miles R. How many subtypes of inhibitory cells in the hippocampus? Neuron. 1998; 20:983–993. [PubMed: 9620702]

Pawelzik H, Hughes DI, Thomson AM. Physiological and morphological diversity of immunocytochemically defined parvalbumin- and cholecystokinin-positive interneurones in CA1 of the adult rat hippocampus. J Comp Neurol. 2002; 443:346–367. [PubMed: 11807843]

Price CJ, Cauli B, Kulik ERKA, Lambolez B, Shigemoto R, Capogna M. Neurogliaform neurons form a novel inhibitory network in the hippocampal CA1 area. J Neurosci. 2005; 25:6775–6786. [PubMed: 16033887]

Ratzliff A, Soltesz I. Differential immunoreactivity for α-actinin-2, an N-methyl-D-aspartate-receptor/actin binding protein, in hippocampal interneurons. Neuroscience. 2001; 103:337–349. [PubMed: 11246149]

Ropireddy D, Ascoli G. Potential Synaptic Connectivity of Different Neurons onto Pyramidal Cells in a 3D Reconstruction of the Rat Hippocampus. Front Neuroinform. 2011; 5:5. [PubMed: 21779242]

Santhakumar V, Aradi I, Soltesz I. Role of Mossy Fiber Sprouting and Mossy Cell Loss in Hyperexcitability: A Network Model of the Dentate Gyrus Incorporating Cell Types and Axonal Topography. J Neurophysiol. 2005; 93:437–453. [PubMed: 15342722]

Schneider CJ, Bezaire M, Soltesz I. Toward a full-scale computational model of the rat dentate gyrus. Front Neural Circ. 2012; 6:83.

Sik A, Penttonen M, Ylinen A, Buzsaki G. Hippocampal CA1 interneurons: an in vivo intracellular labeling study. J Neurosci. 1995; 15:6651–6665. [PubMed: 7472426]

Sik A, Tamamaki N, Freund T. Complete axon arborization of a single CA3 pyramidal cell in the rat hippocampus, and its relationship with postsynaptic parvalbumin-containing interneurons. Eur J Neurosci. 1993; 5:1719–1728. [PubMed: 8124522]

Sik A, Ylinen A, Penttonen M, Buzsaki G. Inhibitory CA1-CA3-hilar region feedback in the hippocampus. Science. 1994; 265:1722–1724. [PubMed: 8085161]

Slomianka L, Amrein I, Knuesel I, Sorensen J, Wolfer D. Hippocampal pyramidal cells: the reemergence of cortical lamination. Brain Struct Funct. 2011; 216:301–317. [PubMed: 21597968]

Slomianka L, West M. Estimators of the precision of stereological estimates: an example based on the CA1 pyramidal cell layer of rats. Neuroscience. 2005; 136:757–767. [PubMed: 16344149]

Soltesz, I. Diversity in the Neuronal Machine: Order and Variability in Interneuronal Microcircuits. New York: Oxford University Press; 2006. p. 264

Somogyi J, Baude A, Omori Y, Shimizu H, Mestikawy SE, Fukaya M, Shigemoto R, Watanabe M, Somogyi P. GABAergic basket cells expressing cholecystokinin contain vesicular glutamate transporter type 3 (VGLUT3) in their synaptic terminals in hippocampus and isocortex of the rat. Eur J Neurosci. 2004; 19:552–569. [PubMed: 14984406]

Somogyi J, Szabo A, Somogyi P, Lamsa K. Molecular analysis of ivy cells of the hippocampal CA1 stratum radiatum using spectral identification of immunofluorophores. Front Neural Circ. 2012; 6

Somogyi P, Klausberger T. Defined types of cortical interneurone structure space and spike timing in the hippocampus. J Physiol. 2005; 562:9–26. [PubMed: 15539390]

Sotty F, Danik M, Manseau F, Laplante F, Quirion R, Williams S. Distinct electrophysiological properties of glutamatergic, cholinergic and GABAergic rat septohippocampal neurons: novel implications for hippocampal rhythmicity. J Physiol. 2003; 551:927–943. [PubMed: 12865506]

Szabadics J, Soltesz I. Functional specificity of mossy fiber innervation of GABAergic cells in the hippocampus. J Neurosci. 2009; 29:4239–4251. [PubMed: 19339618]

Szabo A, Somogyi J, Cauli B, Lambolez B, Somogyi P, Lamsa K. Calcium-permeable AMPA receptors provide a common mechanism for LTP in glutamatergic synapses of distinct hippocampal interneuron types. J Neurosci. 2012; 32:6511–6516. [PubMed: 22573673]

Takacs VT, Freund TF, Gulyas AI. Types and synaptic connections of hippocampal inhibitory neurons reciprocally connected with the medial septum. Eur J Neurosci. 2008; 28:148–164. [PubMed: 18662340]

Takacs VT, Klausberger T, Somogyi P, Freund TF, Gulyas AI. Extrinsic and local glutamatergic inputs of the rat hippocampal CA1 area differentially innervate pyramidal cells and interneurons. Hippocampus. 2012; 22:1379–1391. [PubMed: 21956752]

Tamas G, Lorincz A, Simon A, Szabadics J. Identified sources and targets of slow inhibition in the neocortex. Science. 2003; 299:1902–1905. [PubMed: 12649485]

Toth K, Freund T. Calbindin D28k-containing nonpyramidal cells in the rat hippocampus: their immunoreactivity for GABA and projection to the medial septum. Neuroscience. 1992; 49:793–805. [PubMed: 1279455]

Tricoire L, Pelkey K, Daw M, Sousa V, Miyoshi G, Jeffries B, Cauli B, Fishell G, McBain C. Common origins of hippocampal ivy and nitric oxide synthase expressing neurogliaform cells. J Neurosci. 2010; 30:2165–2176. [PubMed: 20147544]

Tricoire L, Vitalis T. Neuronal nitric oxide synthase expressing neurons: a journey from birth to neuronal circuits. Front Neural Circ. 2012; 6

Van Strien N, Cappaert N, Witter M. The anatomy of memory: an interactive overview of the parahippocampal-hippocampal network. Nat Rev Neurosci. 2009; 10:272–282. [PubMed: 19300446]

Varga C, Golshani P, Soltesz I. Frequency-invariant temporal ordering of interneuronal discharges during hippocampal oscillations in awake mice. Proc Natl Acad Sci U S A. 2012

Varga V, Losonczy A, Zemelman B, Borhegyi Z, Nyiri G, Domonkos A, Hangya B, Holderith N, Magee J, Freund T. Fast synaptic subcortical control of hippocampal circuits. Science Sig. 2009; 326:449.

Vida I, Halasy K, Szinyei C, Somogyi P, Buhl EH. Unitary IPSPs evoked by interneurons at the stratum radiatum-stratum lacunosum-moleculare border in the CA1 area of the rat hippocampus in vitro. J Physiol. 1998; 506:755–773. [PubMed: 9503336]

West MJ, Slomianka L, Gundersen HJG. Unbiased stereological estimation of the total number of neurons in the subdivisions of the rat hippocampus using the optical fractionator. Anat Rec. 1991; 231:482–497. [PubMed: 1793176]

Witter M, Griffioen A, Jorritsma-Byham B, Krijnen J. Entorhinal projections to the hippocampal CA1 region in the rat: an underestimated pathway. Neurosci Lett. 1988; 85:193–198. [PubMed: 3374835]

Wittner L, Henze D, Zaborszky L, Buzsaki G. Three-dimensional reconstruction of the axon arbor of a CA3 pyramidal cell recorded and filled in vivo. Brain Struct Funct. 2007; 12:75–83. [PubMed: 17717699]

Woodson W, Nitecka L, Ben-Ari Y. Organization of the GABAergic system in the rat hippocampal formation: a quantitative immunocytochemical study. J Comp Neurol. 1989; 280:254–271. [PubMed: 2925894]

Wouterlood F, Saldana E, Witter M. Projection from the nucleus reunions thalami to the hippocampal region: light and electron microscopic tracing study in the rat with the anterograde tracer Phaseolus vulgaris-leucoagglutinin. J Comp Neurol. 1990; 296:179–203. [PubMed: 2358531]

Wyeth MS, Zhang N, Mody I, Houser CR. Selective reduction of cholecystokinin-positive basket cell innervation in a model of temporal lobe epilepsy. J Neurosci. 2010; 30:8993–9006. [PubMed: 20592220]

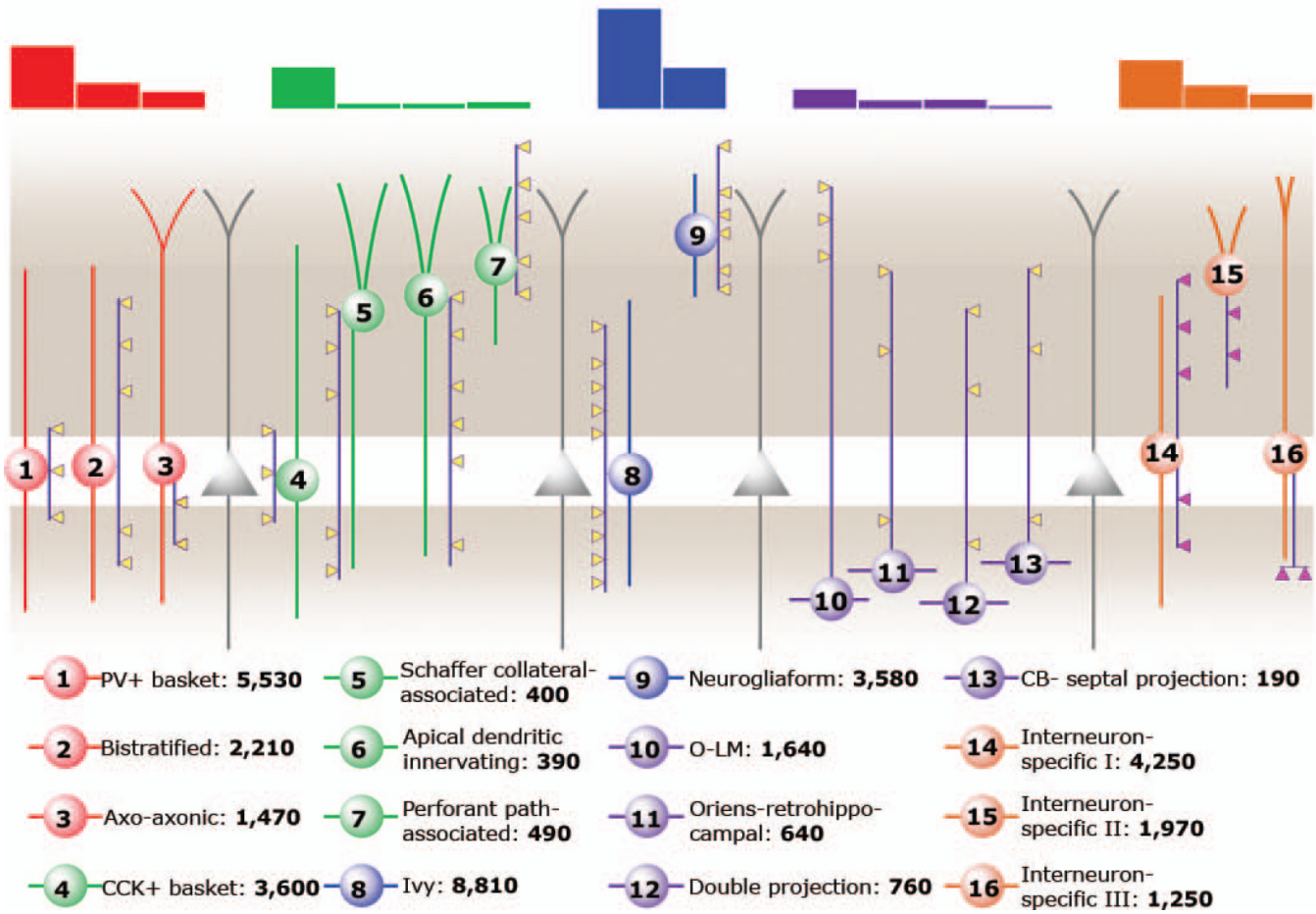

Figure 1.

Diagram of interneuron types included in this work. The top of the diagram shows shows bar graphs illustrating the relative numbers of interneuronal subtypes. The dendrites and somata of the interneurons are the same color, and the axon is shown in purple with color coded boutons. Pink boutons specify synapses made only onto other interneurons. The legend below the diagram gives the names and numbers of each interneuron type. Groups of neurons (CCK+ misc, other SOM+, other) that cannot be objectively subdivided at this time, due to lack of sufficient data, are not depicted here. Figure adapted from: Klausberger T, Somogyi P. 2008. Neuronal diversity and temporal dynamics: the unity of hippocampal circuit operations. Science 321:53–57. Reprinted with permission from AAAS.

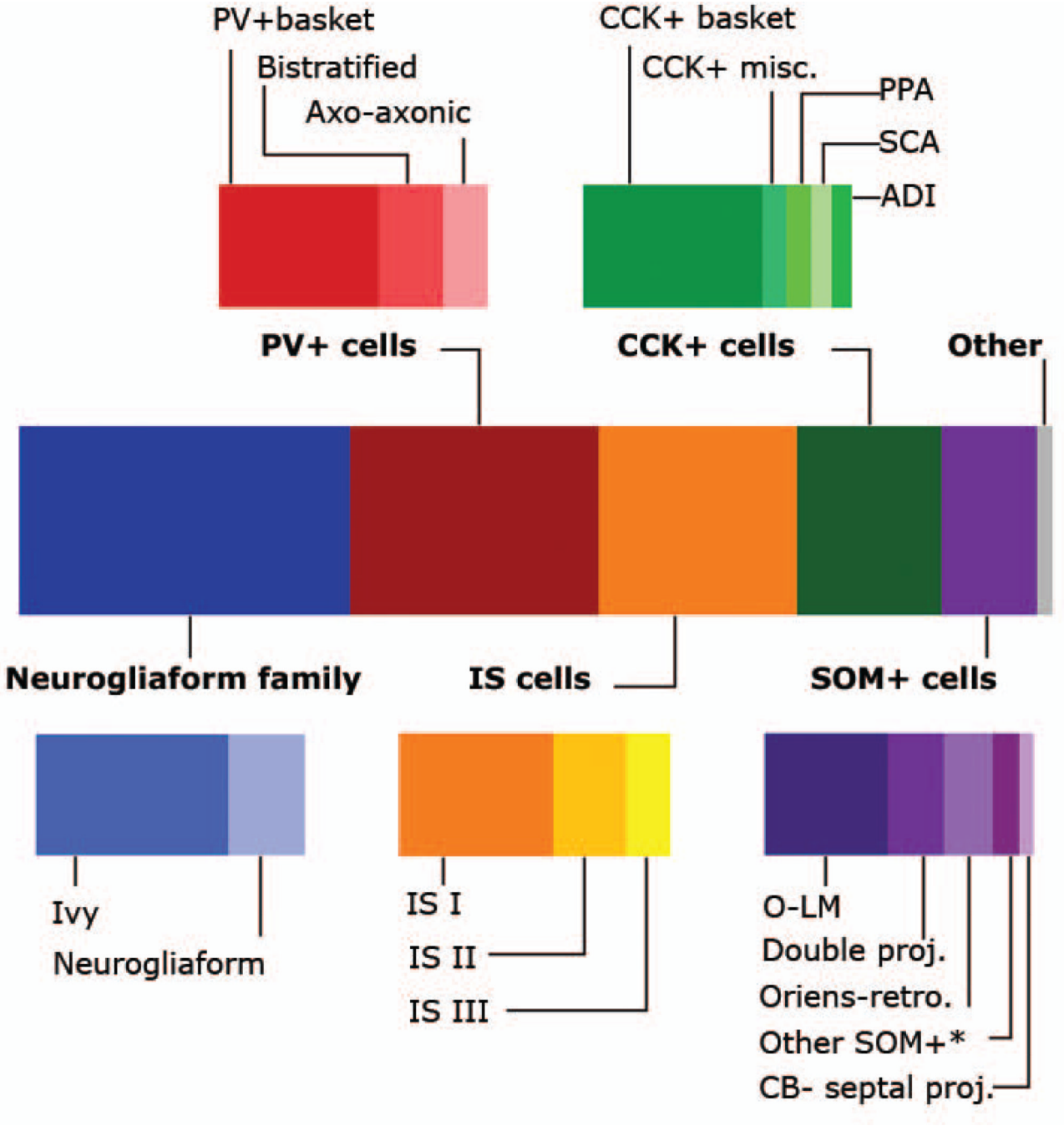

Figure 2.
Bar graph showing the relative proportion of each category and type of interneuron calculated in this work. * Other SOM+ category does not include bistratified cells, although they are known to express SOM.

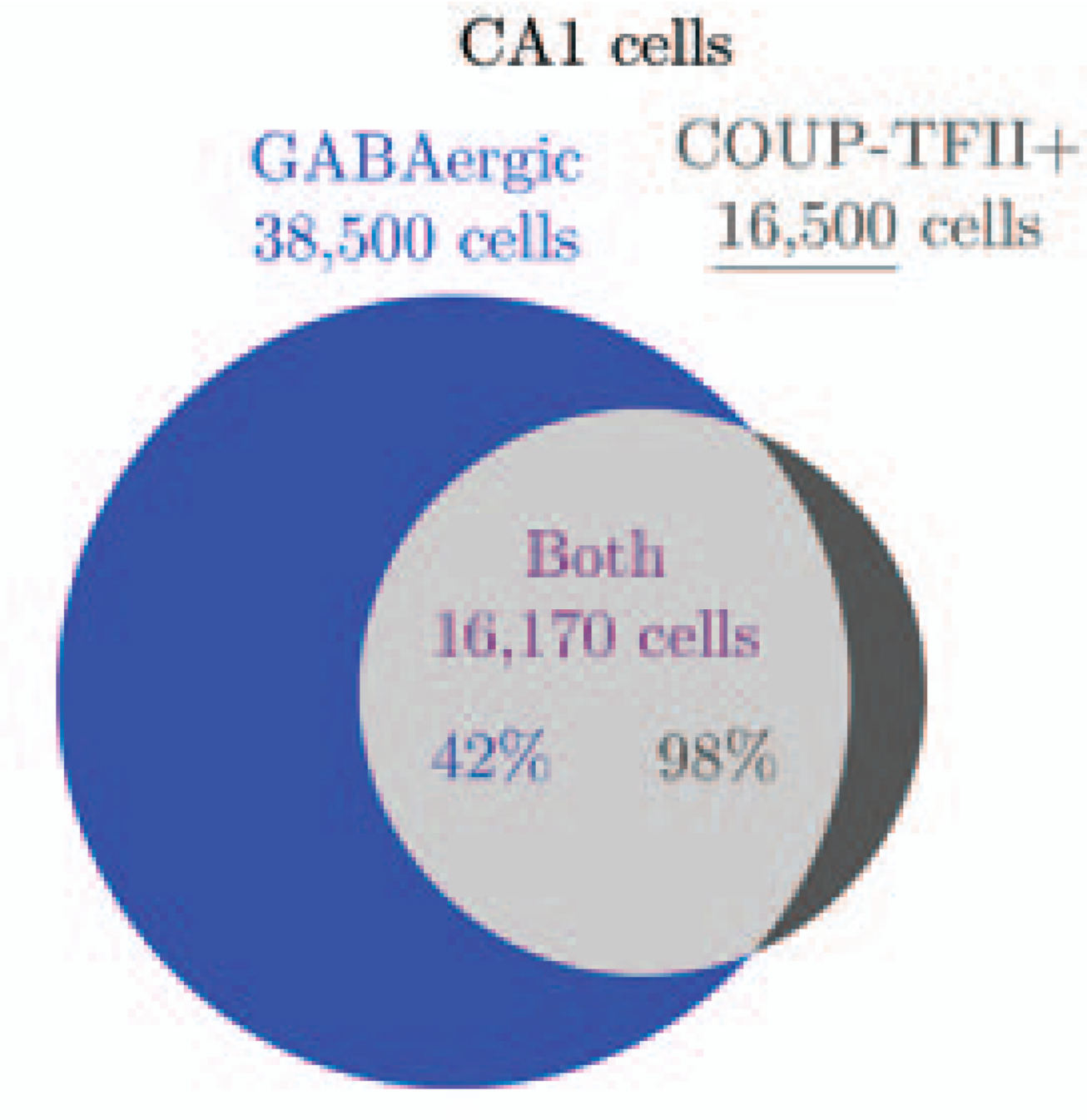

Figure 3.
Venn diagram showing how the number of COUP-TFII expressing cells in the CA1 was calculated. Known data: 42% of GABAergic cells express COUP-TFII and 98% of COUP-TFII cells are GABAergic (Fuentealba et al., 2010); 38,500 of CA1 cells are GABAergic (Table 2). Derived data: total number of COUPTFII+ cells in the CA1 (16,500). We then used the calculated number of COUP-TFII+ cells to estimate the abundance of other classes of cells.

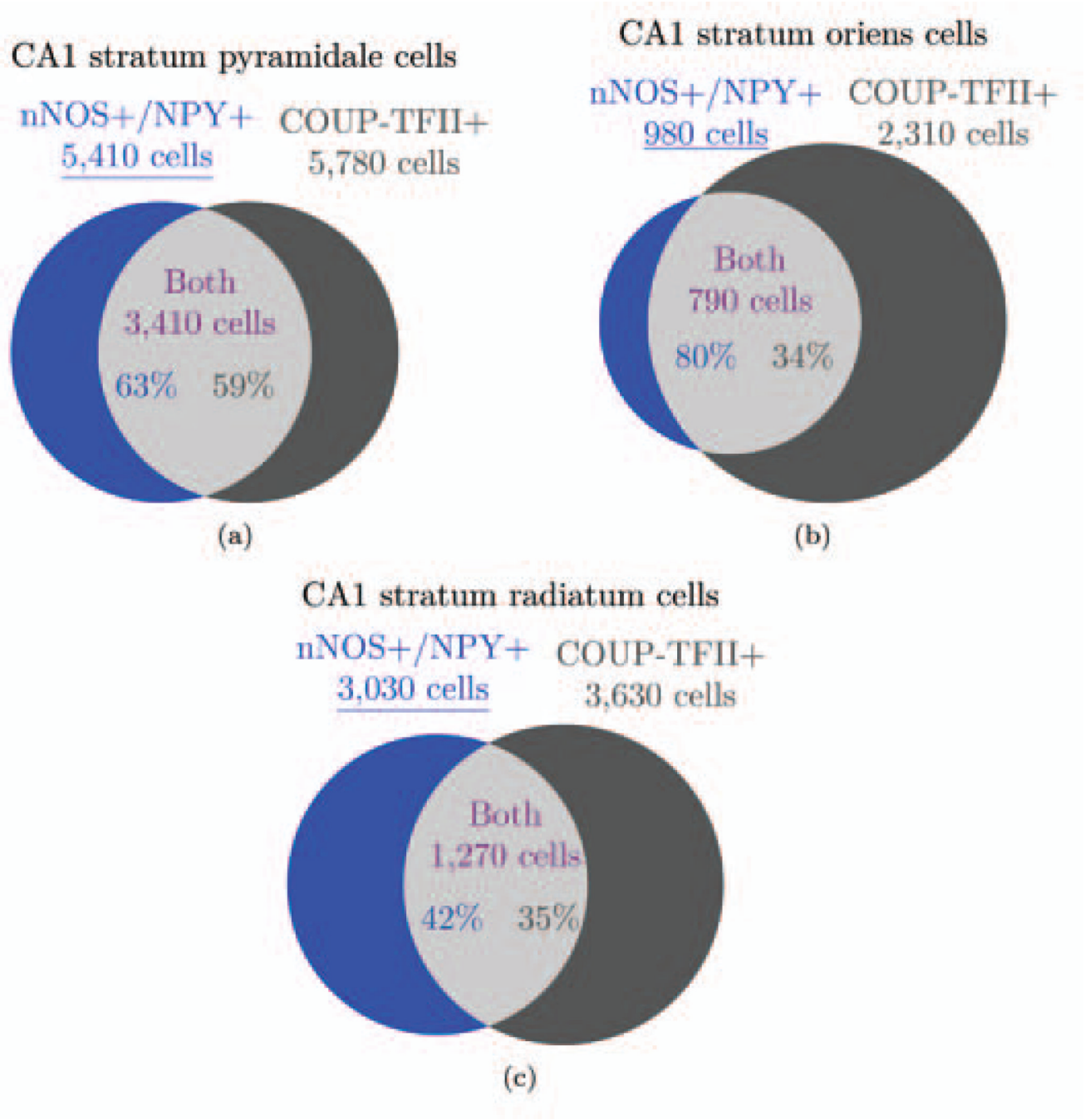

Figure 4.

Venn diagram showing the logic used to obtain the number of nNOS+/NPY+ cells in the CA1 strata oriens, pyramidale, and radiatum. We used the number of COUP-TFII cells in each layer and the percentage of overlap relative to each population (Fuentealba et al., 2010, see their suppl. table 2) to calculate the total number of nNOS+/NPY+/COUP-TFII+ cells and then the number of nNOS+/NPY+ cells (underlined) for each layer.

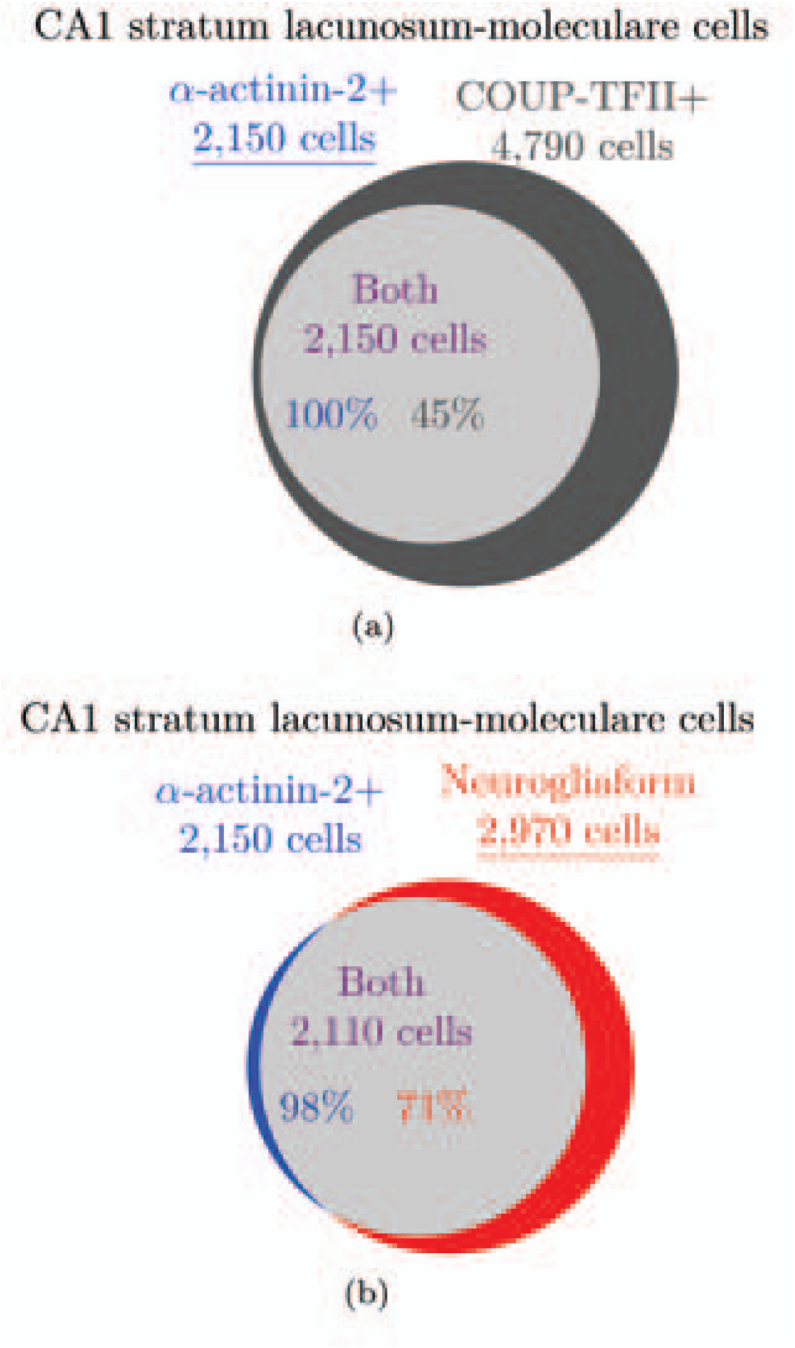

Figure 5.

Venn diagram showing the α-actinin-2-based logic used to obtain the number of neurogliaform cells in the CA1 stratum lacunosum-moleculare. a) Given the number of COUP-TFII cells in the stratum lacunosum and the percentages of overlap (Fuentealba et al., 2010), the total number of α-actinin-2+/COUPTFII+ and α-actinin-2+ cells can be calculated. b) Given the total number of α-actinin-2+ cells and the percentage that are likely to be neurogliaform cells (Price et al., 2005), the total number of neurogliaform cells can be calculated.

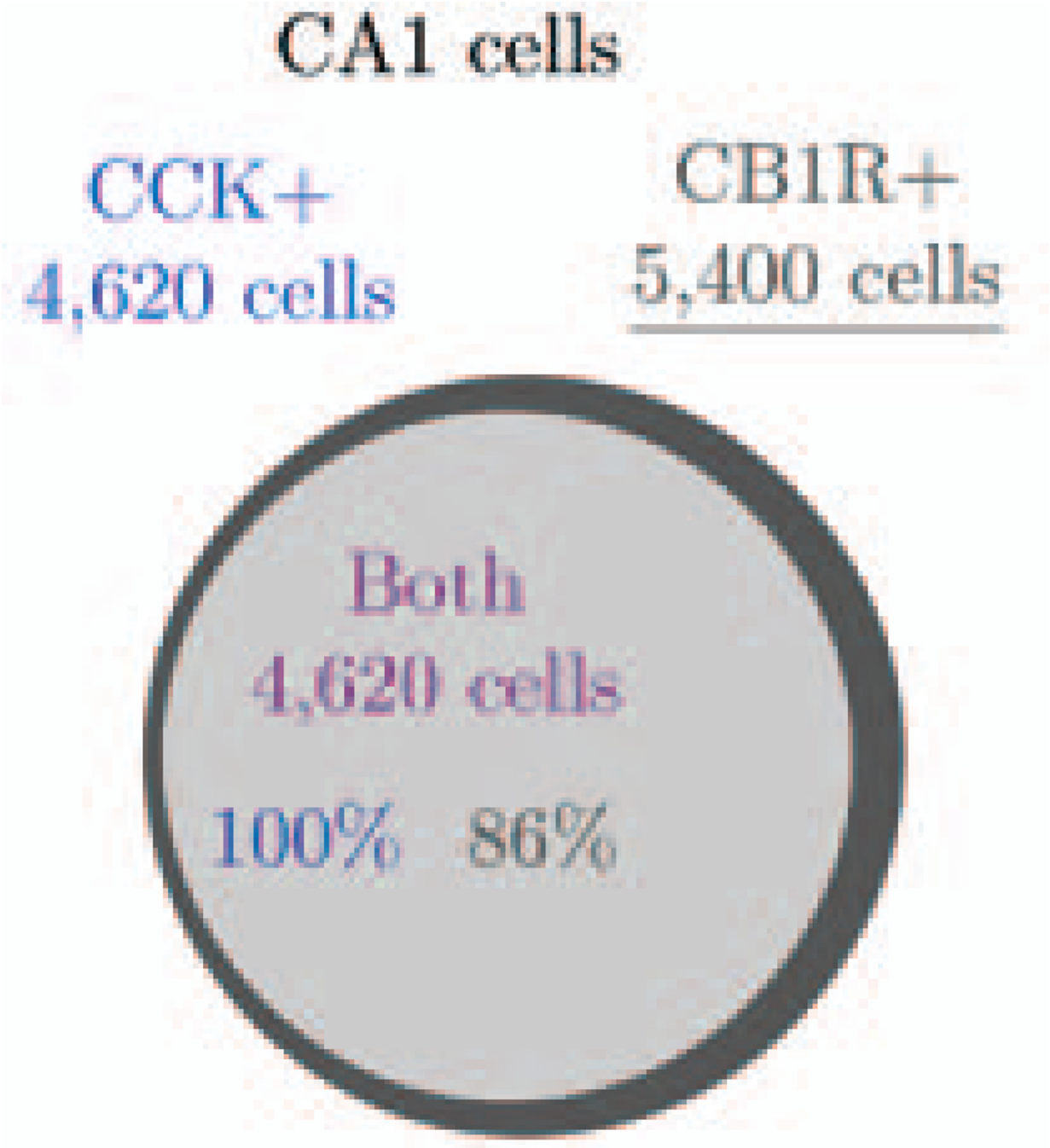

Figure 6.
Venn diagram showing how the number of CB1R expressing cells in the CA1 was calculated. Known data: 100% of CCK+ cells express CB1R and 86% of CB1R+ cells express CCK (Katona et al., 1999b). Derived data: total number of CB1R+ cells in the CA1 (5,400).

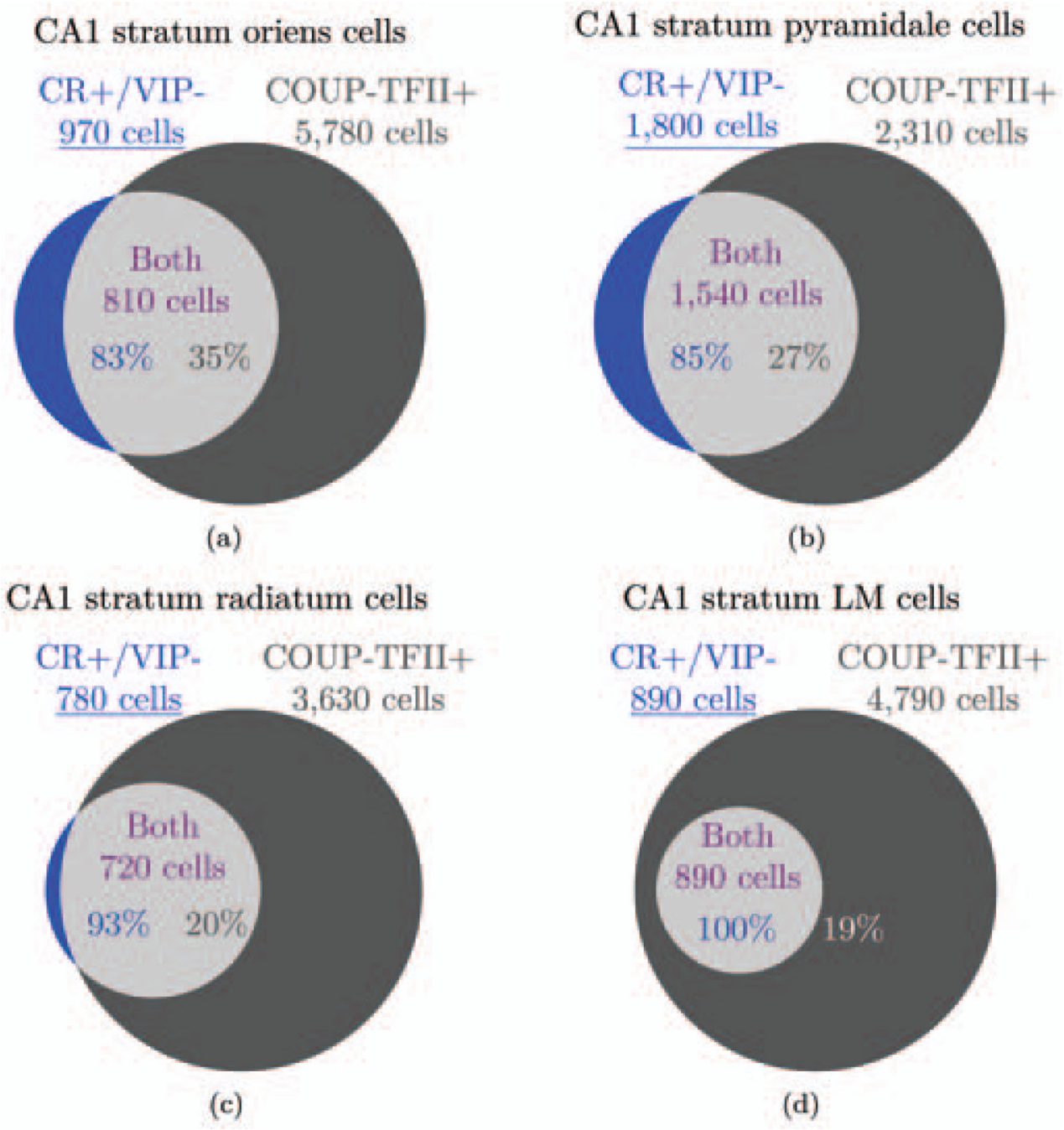

Figure 7.
Venn diagram showing the logic used to obtain the number of CR+/VIP- cells in each layer of the CA1. Given the number of COUP-TFII cells in that layer and the percentage of overlap relative to each population (Fuentealba et al., 2010, see their suppl. table 2), the total number of CR+/VIP-/COUP-TFII+ cells and then the number of CR+/VIP- cells (underlined) was calculated for each layer.

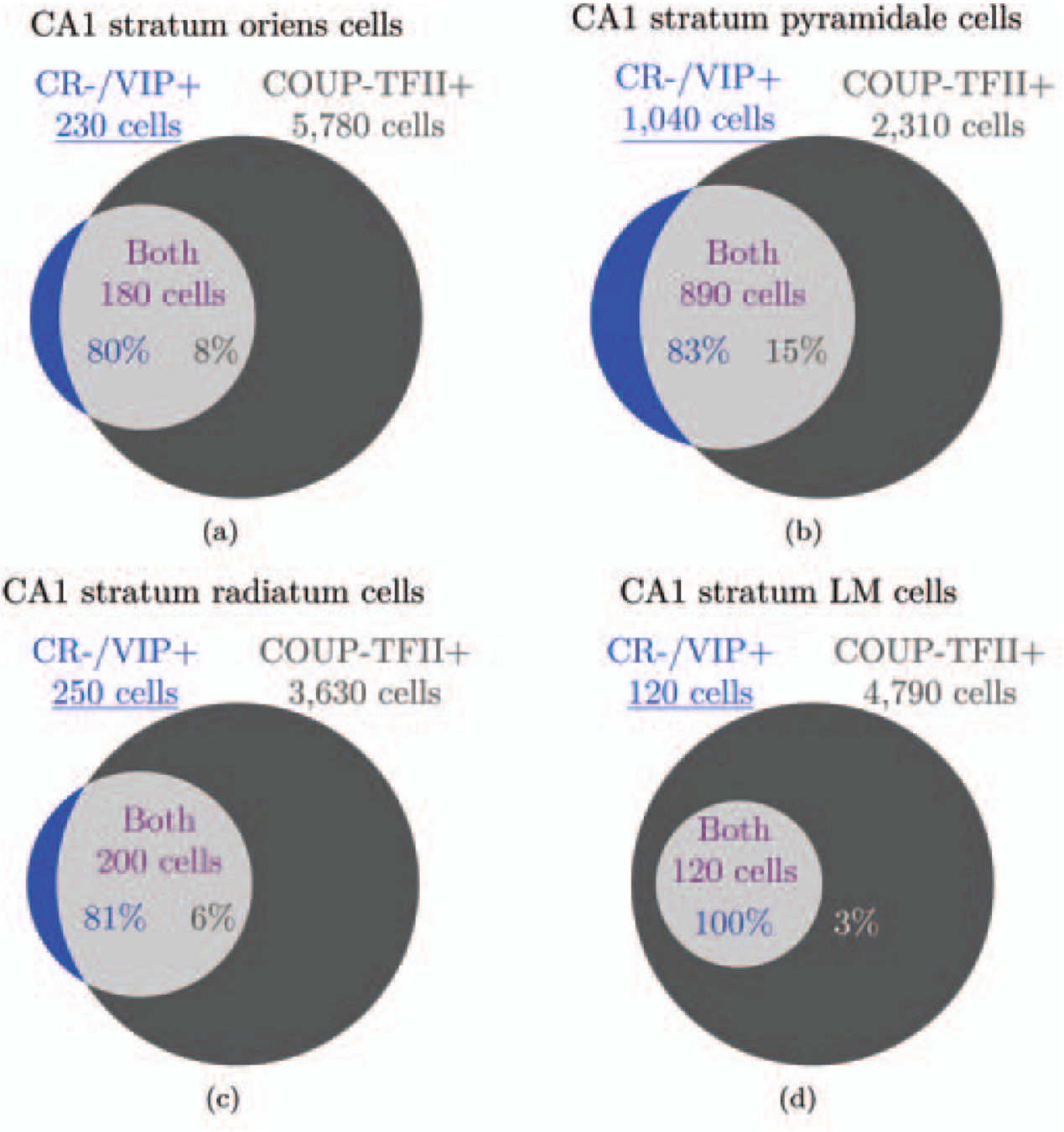

Figure 8.

Venn diagram showing the logic used to obtain the number of CR-/VIP+ cells in each layer of the CA1. Given the number of COUP-TFII cells in that layer and the percentage of overlap relative to each population (Fuentealba et al., 2010, see their suppl. table 2), the total number of CR-/VIP+/COUP-TFII+ cells and then the number of CR-/VIP+ cells (underlined) was calculated for each layer.

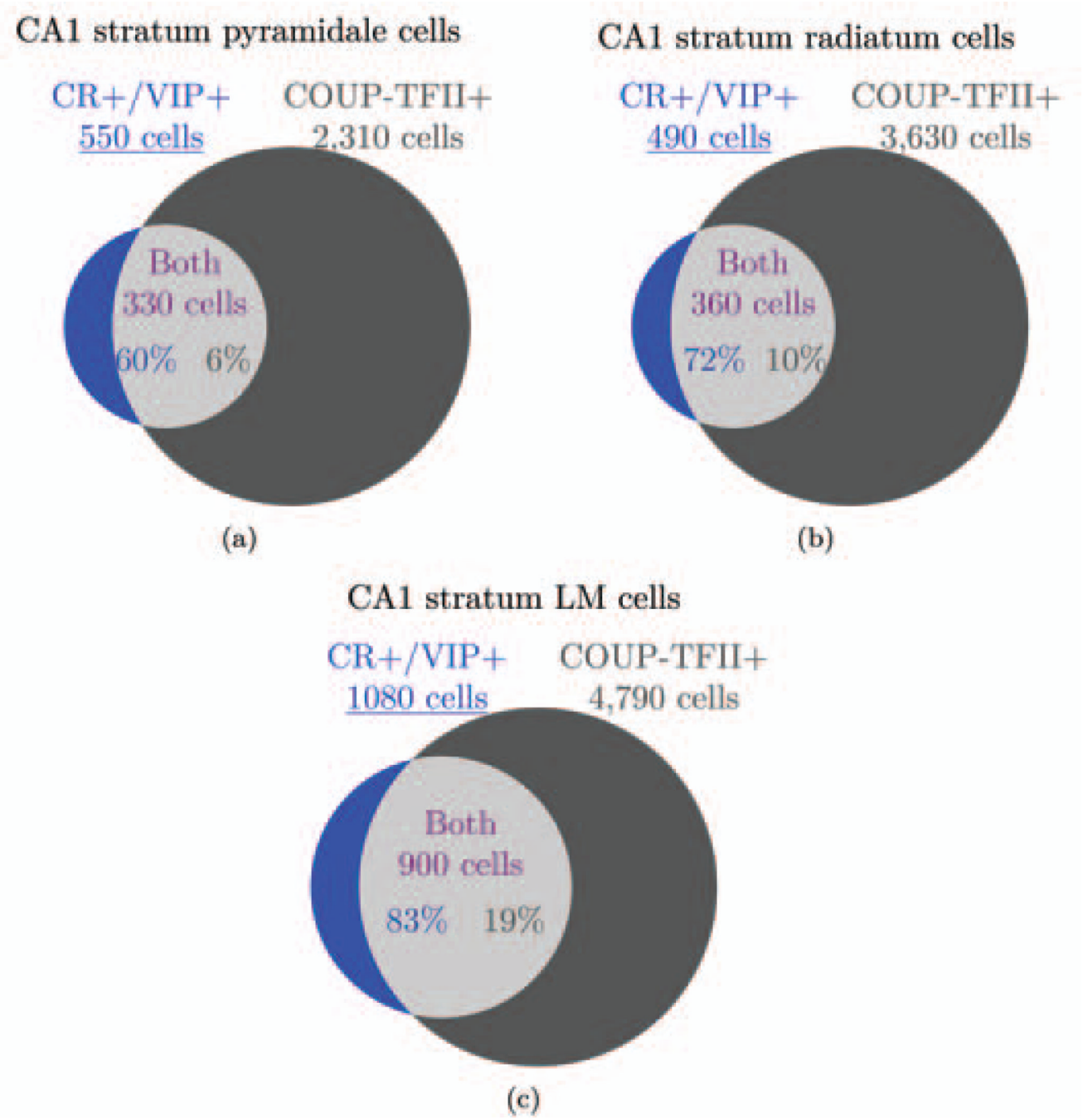

Figure 9.

Venn diagram showing the logic used to obtain the number of CR+/VIP+ cells in each layer of the CA1. Given the number of COUP-TFII cells in that layer and the percentage of overlap relative to each population (Fuentealba et al., 2010, see their suppl. table 2), the total number of CR+/VIP+/COUP-TFII+ cells and then the number of CR+/VIP+ cells (underlined) was calculated for each layer.

Table 1

List of abbreviations for neurochemical markers, cell types, and CA1 strata.

Marker	**Long name**
CB	calbindin
CB1R	CB1 cannabinoid receptor
CCK	cholecystokinin
CR	calretinin
COUP-TFII	COUP transcription factor 2
M2R	muscarinic acetylcholine receptor type 2
mGluR1α	metabotropic glutamate receptor type 1α
mGluR8	metabotropic glutamate receptor type 8
nNOS	neuronal nitric oxide synthase
NPY	neuropeptide Y
PV	parvalbumin
SOM	somatostatin
VIP	vasoactive intestinal polypeptide
Cell type	**Long name**
ADI	Apical dendritic innervating
IS	Interneuron specific
PPA	Perforant path-associated
SCA	Schaffer Collateral-associated
Layer	**Layer name**
SO	stratum oriens
SP	stratum pyramidale
SR	stratum radiatum
SLM	stratum lacunosum-moleculare

Table 2

List of explicit assumptions we were compelled to make to complete our assessment. Related assumptions are grouped together; explanatory text accompanies each assumption. The section numbers of the assessment where the assumptions were made are also included.

#	Explicit, Forced Assumption	Section
1	**11% of CA1 and CA3 cells are GABAergic interneurons.** Experimental observations range from 7–11% (Woodson et al., 1989; Aika et al., 1994). We chose 11% for this assessment after calculating the number of boutons each interneuron would be required to have for all the interneurons to fully cover the GABAergic synapses on all the pyramidal cells.	3.1
2	**CA1 pyramidal cells are homogeneous.** CA1 pyramidal cells vary in many properties as a function of factors such as dorsal/ventral location and depth within the pyramidal layer, for example (Mizuseki et al., 2011; Slomianka et al., 2011; Graves et al., 2012). However, in the absence of detailed quantitative information about how the bouton count and dendritic structure of the pyramidal cells varies with these factors, we have considered the bouton counts of a few CA1 pyramidal cells as representative of all pyramidal cells (Esclapez et al., 1999).	3.1.1
3	**Each CA1 pyramidal cell synapses only once onto each postsynaptic CA1 pyramidal cell.**	3.1.1
4	**Each CA1 pyramidal cell connection onto a CA1 interneuron comprises three synapses.** We made these assumptions to determine the divergence of each CA1 pyramidal cell. Deuchars and Thomson (1996) studied the anatomy of one pyramidal to pyramidal cell pair that was found to have two synapses, but its EPSP amplitude was over twice that of the average and so we concluded that most pyramidal to pyramidal connections comprise one synapse. For the CA1 pyramidal cell to interneuron connections, we based our assumption on an observation that CA1 pyramidal cells generally contact O-LM cells with three synapses each (Biro et al., 2005). However, in the CA3, some pyramidal cell to basket cell connections were observed to include only one synapse (Sik et al., 1993; Gulyas et al., 1993) and the EPSP amplitude range of these connections (Gulyas et al., 1993) was similar to that seen in connections in the CA1 (Ali et al., 1998). Yet, current clamp recordings of pyramidal cell to interneuron connections (bistratified and basket cells) in the CA1 revealed a large enough range in EPSP amplitude to suggest that at least some connections may comprise multiple synapses, especially connections onto bistratified cells (Ali et al., 1998).	3.1.1
5	**Observations made in the dorsal CA1 are representative of the whole CA1.**	2.2
6	**The expression of COUP-TFII in interneurons dorsally is representative of the whole CA1.** Some properties (marker expression, frequency of certain cell types) vary between dorsal and ventral CA1 (Kosaka et al., 1987; Nomura et al., 1997a,b; Fuentealba et al., 2010). Where possible, we averaged values from both sides. In some cases, only dorsal area observations were available. Therefore, our findings will be more representative of the dorsal CA1.	3.1.2
7	**All nNOS+/NPY+ cells are either ivy cells or neurogliaform cells.**	3.1.2
8	**All nNOS+/NPY+ cells with somata in the stratum oriens or pyramidale are ivy cells.**	3.1.2
9	**nNOS+/NPY+/reelin+ cells in the stratum radiatum are neurogliaform cells.**	3.1.2
10	**nNOS+/NPY+/reelin− cells in the stratum radiatum are ivy cells.**	3.1.2
11	**All ivy cells are nNOS+/NPY+ with somata in the stratum oriens, pyramidale, or radiatum.**	3.1.2
12	**All α-actinin-2+/CR− cells in the stratum lacunosum-moleculare are neurogliaform cells.** We considered nNOS and NPY to generally indicate neurogliaform family cells (Price et al., 2005; Fuentealba et al., 2010), though we resorted to different criteria in the stratum lacunosum-moleculare because some nNOS+/NPY+ cells there were found to not be neurogliaform family cells (Price et al. 2005). Ivy and neurogliaform cells have similar marker expression profiles (see Armstrong et al., 2012), so we separated them by layer and reelin expression.	3.1.2
13	**Ivy and neurogliaform cells make 10 classical synapses on each postsynaptic cell.** Most neurogliaform family cell boutons do not participate in classical synapses (i.e., do not have a corresponding postsynaptic element) but instead rely on volume transmission (Olah et al., 2009, in somatosensory cortex). For our convergence calculations, we found it necessary to assume a number of corresponding postsynaptic elements (classical synapses) for each connection. We based this number on a prediction made about classical synapses on observations of neurogliaform cell to pyramidal cell connections in the neocortex (Tamas et al., 2003).	3.1.2
14	**All stratum oriens SOM+/CB+ cells projecting to the septum are double projection cells.**	3.1.3

#	Explicit, Forced Assumption	Section
	Double projection cells are known to express SOM and CB and to project to the septum (Toth and Freund, 1992; Somogyi and Klausberger, 2005; Jinno et al., 2007). Though there appear to be other, minor groups projecting to the septum (Hajos and Mody, 1997; Katona et al., 1999a; Ferraguti et al., 2005; Jinno, 2009), they have not been shown to express SOM and CB together.	
15	**All SOM+ cells projecting to the subiculum are either double projection or oriens-retrohippocampal cells.** Of the projection cells, four types are known to target the subiculum: double projection, oriens-retrohippocampal, radiatum-retrohippocampal, and trilaminar (Klausberger and Somogyi, 2008). We separated these into two groups by their SOM expression.	3.1.3
16	**Projection interneurons of the stratum oriens with axons in strata oriens and radiatum have the same number of local boutons as do the so-called back projection cells.**	3.1.3
17	**Projection interneurons of the stratum oriens with axons in strata oriens and radiatum have the same laminar distribution of local boutons as do conventional bistratified cells.** For several projection cell types, their cell numbers could be estimated but we had no direct observations of their bouton counts or distribution. Because their axon arbors are similar to those of the so-called back projection cells (both the laminar distribution and the small number of local targets; Sik et al., 1994) and conventional bistratified cells (laminar distribution; Sik et al., 1995), we used information from those types to estimate total bouton counts and distribution respectively, which enabled us to calculate local convergence.	3.1.3
18	**All stratum oriens-specific cell types contact their postsynaptic targets with 10 synapses each.** A light microscopy study of O-LM to pyramidal cell connections showed a range of three to 17 potential synapses per connection (Maccaferri et al., 2000). We took the average of 10 synapses per connection, assuming the potential synapses made actual contact. For projection cells whose axons mainly ramify in the strata radiatum and oriens (formerly known as oriens-bistratified cells), a connection was observed to comprise 10 potential synapses (Maccaferri et al., 2000). Therefore, we assumed that all stratum oriens-specific cells contacted their postsynaptic targets with 10 synapses.	3.1.3
19	**The ratio of PV+ basket cells:bistratified cells:axo-axonic cells within the stratum pyramidale is the same as the ratio in other layers.** In the absence of data about the composition of the PV+ cells in the stratum radiatum and oriens, we assumed it was similar to the stratum pyramidale. Though this assumption may favor PV+ basket cells, the majority of PV+ cells are located in the stratum pyramidale, and so we felt observations made in the stratum pyramidale could be treated as broadly representative of PV+ cells in the whole CA1 without introducing significant error.	3.1.4
20	**Axo-axonic cells have an average of 7,200 boutons each.** We based this assumption on the published divergence of a single axo-axonic cell and on the observed number of synapses made for one connection onto a pyramidal cell (Li et al., 1992).	3.1.4
21	**The ratio of PV+:CCK+ basket cell boutons in the entire CA1 is 1.6:1.** We averaged data regarding the relative frequency of PV+ and CCK+ basket cell boutons on pyramidal cell somata and in the pyramidal layer of the mouse CA1 (Foldy et al., 2010; Wyeth et al., 2010). We took this ratio to be representative of the total number of boutons of each basket cell type in rat CA1, for the purpose of calculating the number of CCK+ basket cells.	3.1.5
22	**Only basket cells synapse on the somata of pyramidal cells.** Though other cell types sometimes synapse on pyramidal cell somata, such as bistratified, ivy, or trilaminar cells (Ferraguti et al., 2005; Buhl et al., 1994a; Fuentealba et al., 2008a), we assumed that their contribution was minor in our calculations of interneuronal convergence onto pyramidal cells.	3.3.2
23	**Basket cells in the stratum radiatum are likely CCK+ basket cells.**	3.1.5
24	**CCK+ basket cells are found in all layers of the CA1.** Many CCK+ basket cells are located in the stratum radiatum; therefore, we assumed unlabelled basket cells in the stratum radiatum were representative of CCK+ basket cells. However, CCK+ basket cells are also found in every other layer of the CA1, even in the stratum lacunosum-moleculare (Vida et al., 1998).	3.1.5
25	**CCK+ SCA and ADI cells are only found in the stratum radiatum; all CCK+ cells that are not basket cells in that layer are SCA or ADI cells.**	3.1.5
26	**CCK+ PPA cells are only found in the stratum lacunosum-moleculare; all CCK+ cells that are not basket cells in that layer are PPA cells.**	3.1.5

#	Explicit, Forced Assumption	Section
27	**Of CCK+ cells in the stratum radiatum that are not basket cells, half are SCA cells and half are ADI cells.** To gain a rough idea of the numbers of CCK+ cell types, we identified them based on their characteristic layer (Klausberger and Somogyi, 2008). However, various CCK+ cell types are found in more than one layer. For example, here we assumed that PPA cells were only in the stratum lacunosum-moleculare, but in reality they are occasionally found in the stratum radiatum (Hajos and Mody, 1997) and even once in the stratum oriens (Klausberger et al., 2005).	3.1.5
28	**All CCK+/VIP+ and CCK+/VGLUT3+ GABAergic cells are CCK+ basket cells.** However, ADI cells have been shown to express VGLUT3 (Klausberger et al., 2005), but it is not known what proportion of them express VGLUT3.	3.1.5
29	**CCK+ basket cells do not express CB; all CCK+/CB+ cells are non-basket cell types.**	3.1.5
30	**All the CCK+/CB− cells in the strata oriens and pyramidale are CCK+ basket cells.**	3.1.5
31	**Lesser known CCK+ cell types are found in the strata oriens and pyramidale.** Since no CCK+ basket cells have been found to express CB, we assumed that any CCK+/CB+ cells were not basket cells. Little has been published about the lesser-known CCK+ cell types, so we assumed they made up the remaining non-basket cell types in the strata oriens and pyramidale.	3.1.5
32	**The septotemporal and mediolateral bouton distribution of CCK+ basket cells is the same as for PV+ basket cells.** We made this assumption so that we could extrapolate from the slice data to a full axonal bouton count for CCK+ basket cells, using PV+ basket cell bouton distribution data (Halasy et al., 1996).	3.1.5
33	**CCK basket cells make eight synapses per connection with other interneurons.** We made this assumption because they have been shown to make eight synapses/connection with pyramidal cells in mouse (Foldy et al., 2010). However, it has been shown that PV+ basket cells make only one or a few synapses per connection with interneurons (Sik et al., 1995) despite making many synapses per connection on pyramidal cells (Foldy et al., 2010, in mouse). It is not known whether CCK+ basket cells also display this difference with connections onto interneurons, so we assumed they did not.	3.1.5
34	**SCA cell and PPA cell axons are distributed such that approximately 50% of their boutons are located outside of a 400 μm thick slice containing the soma.** The bouton counts for an SCA cell and for a PPA cell were only available for a 400 μm slice (Vida et al., 1998). To extrapolate this count to a total bouton count for the entire SCA or PPA axon, we compared bouton count data for a bistratified cell in a 400 μm slice (Pawelzik et al. 2002) and in a full axon fill (Sik et al., 1995). We found that, for the bistratified cell, the full axon fill had about double the boutons as the slice, so we assumed the same would be true of the SCA cell axon and the PPA cell axon.	3.1.5
35	**All IS cells express CR or VIP or both.**	3.1.6
36	**All cells that express CR or VIP are IS I, II, or III cells, except for CCK+/VIP+ basket cells and CR+ septally projecting cells.**	3.1.6
37	**CR+/VIP− cells are IS-I or septally projecting cells, CR−/VIP+ cells are IS-II cells, and CR+/VIP+ cells are IS-III cells.**	3.1.6
38	**All VIP+ cells are CCK+/VIP+ basket cells or IS cells.** CR is generally a marker of interneuron specificity, but not all IS cells are known to express CR (Acsady et al., 1996a, 1996b; Gulyas et al., 1996; Somogyi and Klausberger, 2005). Those that do not may express VIP (but so do some basket cells). Therefore, we took CR and VIP to be the most reliable markers of interneuron specificity and considered that the various combinations of the two markers identified different types of IS cells. Enkephalin may also be expressed by IS cells (Fuentealba et al., 2010), but it is also expressed by non-IS cells (Price et al., 2005) so we have not derived any information from its expression.	3.1.6
39	**Approximately 10% of GABAergic cells in the CA1 express calbindin.** It has been previously estimated that 10% of GABAergic cells are CB+ (Freund and Buzsaki, 1996).	3.1.7
40	**Averaging the inputs to the CA1 from a CA3a and CA3c cell represents the inputs from an average CA3 cell.** There are known to be significant differences in bouton count and distribution in pyramidal cells from CA3a and CA3c (Sik et al., 1993; Wittner et al., 2007). Since we had data from both areas, we combined it to calculate the laminar distribution and total CA1 divergence of an average CA3 pyramidal cell.	3.2.1

#	Explicit, Forced Assumption	Section
41	**For those cell types for which their ratio of innervation of pyramidal cells to interneurons is unknown, the bouton target ratio of 92:8 (pyramidal cell:interneuron) is adequate.** We determined the ratio as described in the methods. This ratio took into account the proportion of pyramidal cells and interneurons as well as their numbers of GABAergic input synapses. In reality, the ratio is likely to be even more skewed towards pyramidal cells because some interneurons receive a significant amount of inhibition from afferent GABAergic neurons.	3.1
42	**Unless stated otherwise, the proximally projecting cell types only contact postsynaptic pyramidal cells on the basal dendrites in the stratum oriens and proximal apical dendrites in the stratum radiatum.** Some bistratified cells, ivy, or SCA cells have been shown to make occasional synapses in the strata pyramidale or lacunosum-moleculare (Buhl et al., 1994a; Vida et al., 1998; Szabo et al., 2012), and their contribution to those layers has been quantified here. Those synapses counted as being in the stratum pyramidale, we have assigned to the proximal apical or basal dendrites.	3.3.4
43	**Unless stated otherwise, the distally projecting cell types only contact postsynaptic pyramidal cells on the distal apical dendrites in the stratum lacunosom-moleculare.** This assessment still accounts for some neurogliaform cell boutons in the stratum radiatum (especially because some neurogliaform cells are found in the stratum radiatum, Somogyi et al., 2012) and some O-LM cell boutons in the stratum oriens (Sik et al., 1995), but assumes that PPA cells only synapse in the stratum lacunosum-moleculare since there are no quantitative data about them in other layers.	3.3.5
44	**The entorhinal cortex supplies most of the excitatory inputs to the stratum lacunosum-moleculare.** Though the nucleus reuniens supplies a significant portion of excitatory inputs to the stratum lacunosum-moleculare (Wouterlood et al., 1990), not enough information is yet available to quantify their contribution, so we have assumed that the excitatory inputs to the stratum lacunosum-moleculare are supplied by the entorhinal cortex (Witter et al., 1988).	3.2.1

Table 3

Rat types used in each of the references cited for the quantitative assessment; review articles are not included here. - indicates the information was not provided in the reference.

Reference	Sex	Strain	Age	Weight (grams)
Acsady et al. (1996a)	male	Wistar	2 months	300 – 350
Acsady et al. (1996b)	male	Wistar	-	300 – 350
Aika et al. (1994)	male	Wistar	9 – 10 weeks	280
Ali et al. (1998)	male	-	adult	90 – 180
Armstrong et al. (2011)	both	Wistar	3 – 5 weeks	-
Baude et al. (2007)	male	Sprague Dawley	-	250 – 350
Biro et al. (2005)	male	Wistar	14 – 21 days	-
Borhegyi et al. (2004)	-	-	-	-
Buhl et al. (1994a)	-	-	-	-
Buhl et al. (1994b)	female	Wistar	young	-
Buhl et al. (1995)	female	Wistar	young adult	> 150
Chen et al. (2003)	-	Sprague Dawley	variable	-
Cobb et al. (1997)	female	Wistar	young adult	> 150
Cope et al. (2002)	male	Wistar	juvenile	-
Deuchars and Thomson (1996)	male	Sprague Dawley	-	100 – 180
Elfant et al. (2008)	male	Sprague Dawley	18 – 22 days	-
Esclapez et al. (1999)	male	Wistar	young adult	180 – 200
Ferraguti et al. (2004)	-	Wistar	adult	-
Ferraguti et al. (2005)	-	Wistar	adult	300 – 400
Foldy et al. (2010)	rat and mouse			
Fuentealba et al. (2008a)	male	Sprague Dawley	-	250 – 350
Fuentealba et al. (2008b)	male	Sprague Dawley	adult	200 – 250
Fuentealba et al. (2010)	male	Sprague Dawley	adult	300 – 350
Graves et al. (2012)	male		21 – 28 days	-
Gulyas et al. (1990)	male	CFY	adult	250 – 300
Gulyas et al. (1991)	male	Wistar	-	250
Gulyas et al. (1996)	male	Wistar	-	250
Gulyas et al. (1999)	male	Wistar	-	250
Gulyas et al. (2001)	-	Sprague Dawley	17 – 22 days	-
Gulyas et al. (2003)	male	Wistar	adult	250
Hajos and Mody (1997)	male	Wistar	20 − 28 days	-
Halasy et al. (1996)	female	Wistar	7 – 8 weeks	-
Halasy et al. (2004)	both	Sprague Dawley	adult	250 – 300
Jinno and Kosaka (2006)	mouse			
Jinno et al. (2007)	male	Sprague Dawley	-	250 – 350
Kajiwara et al. (2008)	female	Wistar	-	200 – 220

Reference	Sex	Strain	Age	Weight (grams)
Katona et al. (1999a)	male	Wistar	2 months	300 – 350
Katona et al. (1999b)	male	Wistar	2 months	300 – 350
Klausberger et al. (2004)	male	Sprague Dawley	-	250 – 350
Klausberger et al. (2005)	male	Sprague Dawley	-	250 – 350
Kohler (1985)	male	Sprague Dawley	-	150 – 200
Kosaka et al. (1985)	male	Wistar	5 − 8 weeks	120 – 200
Kosaka et al. (1987)	male	Wistar-Imamichi	5 − 8 weeks	120 – 200
Kosaka et al. (1988)	male	Wistar-Imamichi	5 − 6 weeks	-
Lee et al. (2010)	-	Sprague Dawley	17 – 22 days	-
Li et al. (1992)	both	-	-	-
Li et al. (1994)	both	Sprague-Dawley, Wistar	adult	-
Maccaferri et al. (2000)	-	Wistar	10 – 17 days	-
Matyas et al. (2004)	male	Wistar	-	250
Megias et al. (2001)	male	Wistar	adult	300
Melzer et al. (2012)	mouse			
Miles et al. (1996)	guinea pig			
Miyashita and Rockland (2007)	male	Wistar	adult	-
Mizuseki et al. (2011)	male	Long-Evans	-	250 – 400
Mulders et al. (1997)	female	Wistar	30 days	-
Nomura et al. (1997a)	male	Wistar	5 weeks	85 – 100
Nomura et al. (1997b)	male	Wistar	5 weeks	85 – 100
Olah et al. (2009)	-	Wistar	22 – 35 days	-
Pawelzik et al. (2002)	male	Sprague Dawley	-	120 – 200
Price et al. (2005)	-	Sprague Dawley	12 − 21 days	-
Ratzliff and Soltesz (2001)	-	Wistar	adult	-
Ropireddy and Ascoli (2011)	male	Long-Evans	45 days	226 – 237
Sik et al. (1993)	male	Sprague Dawley	-	200 – 300
Sik et al. (1994)	-	-	-	-
Sik et al. (1995)	-	Sprague Dawley	-	250 – 350
Slomianka and West (2005)	male	Wistar	-	305 – 315
Somogyi et al. (2004)	male	Wistar	-	150 – 250
Somogyi et al. (2012)	male	Sprague Dawley	3 − 4 weeks	-
Sotty et al. (2003)	-	Sprague Dawley	13 – 19 days	-
Szabadics and Soltesz (2009)	-	-	21 – 30 days	-
Szabo et al. (2012)	-	Sprague Dawley	3 – 4 weeks	-
Takacs et al. (2008)	male	Wistar	>1 month	200 – 300
Takacs et al. (2012)	female	Wistar	-	> 110
Tamas et al. (2003)	-	Wistar	19 – 35 days	-
Toth and Freund (1992)	male	Wistar	adult	250

Reference	Sex	Strain	Age	Weight (grams)
Tricoire et al. (2010)	mouse			
Varga et al. (2012)	mouse			
Vida et al. (1998)	female	Wistar	young adult	> 120
West et al. (1991)	-	Wistar	30 days	-
Witter et al. (1988)	female	Wistar	-	180 – 200
Wittner et al. (2007)	-	Sprague Dawley	-	-
Woodson et al. (1989)	-	Wistar	adult	-
Wouterlood et al. (1990)	female	Wistar	young adult	180 – 250
Wyeth et al. (2010)	mouse			

Table 4

Estimated number of each type of interneuron. The fraction is computed on the basis of 38,500 interneurons. Note that this table does not include some cell types for which little information is known. Also, the interneurons in the “other interneurons” category do not count towards any of the laminar totals.

Interneuron Type	Fraction	Total	Layer			
			SO	SP	SR	SLM
Neurogliaform Family	**32.2%**	**12,390**	**980**	**5,410**	**3,030**	**2,970**
Ivy	22.9%	8,810	980	5,410	2,420	0
Neurogliaform	9.3%	3,580	0	0	610	2,970
SOM Expressing	**9.3%**	**3,580**	**3,580**	**0**	**0**	**0**
O-LM	4.3%	1,640	1,640	0	0	0
Double Projection	2.0%	760	760	0	0	0
CB− septal proj.	0.5%	190	190	0	0	0
Oriens-retrohipp.	1.7%	640	640	0	0	0
Other SOM+ cells *	0.9%	350	350	0	0	0
PV Expressing	**23.9%**	**9,210**	**2,200**	**6,460**	**550**	**0**
PV+ Basket	14.4%	5,530	1,320	3,880	330	0
Bistratified	5.7%	2,210	530	1,550	130	0
Axo-axonic	3.8%	1,470	350	1,030	90	0
CCK Expressing	**13.9%**	**5,370**	**1,140**	**1,070**	**1,960**	**1,200**
CCK+ Basket	9.4%	3,600	780	940	1,170	710
ADI	1.0%	390	0	0	390	0
SCA	1.0%	400	0	0	400	0
PPA	1.3%	490	0	0	0	490
CCK Misc.	1.3%	490	360	130	0	0
Interneuron-Specific	**19.4%**	**7,470**	**780**	**3,190**	**1,450**	**2,050**
IS I	11.0%	4,250	780	1,800	780	890
IS II	5.1%	1,970	0	480	450	1,040
IS III	3.2%	1,250	0	910	220	120
Other Interneurons	**1.2%**	**480**				
Total Interneurons	**100%**	**38,500**	**8,680**	**16,130**	**6,990**	**6,220**

* The Other SOM+ Cells category has the number of PV+ bistratified cells in the stratum oriens subtracted, since most of these cells are likely to express SOM.

Table 5

Bouton counts and laminar distribution, along with divergence, for various interneuron types. The 'density' column gives the average bouton density of the axon. Total axonal length and bouton counts refer to local (CA1 area) only. The Divergence:Connections columns are all calculated from other data in the table.

	Axonal			Classical Boutons		Laminar Distribution (%)				Divergence				
	Extent	Length	Density							Fraction (%)		Connections		
Cell	(mm)	(μm)	(/100 μm)	Total	Syn.s /conn	SO	SP	SR	SLM	Pyr.	Inrn.	Total	Pyr.	Inrn.
Ivy	ML: 0.75[e]	176,760[c,e]	41.7[a,c,t,u]	16,200[c]	10[a,q]	40	2	50	8[c,e,p]	92	8[a]	1,620	1,490	130
	RC: 1.31[e]													
Neuroglia-form	ML: 0.5[d]	144,000[c]	41.7[a,c,t,u]	13,200[c]	10[a,q]	0	0	17	83[c]	92	8[a]	1,320	1,214	106
	ST: 1.2[d]													
O-LM	ML: 0.50[f]	62,490[f]	26.6[f]	16,370[c,f]	10[s]	7	0	0	93[c,f]	89	11[c,o]	1,637	1,457	180
	ST: 0.84[f]													
Double proj.				6,080[a,h]	10[s]	58	0	42	0[a,c,f]	92	8[c,i,v]	608	559	49
Oriens retrohipp.				6,080[a,h]	10[s]	58	0	42	0[a,c,f]	96	4[i]	608	584	24
Trilaminar	ML: 2.45[f]	54,740[f]	28.2[f]	15,440[c,f]	10[s]	13	17	70	0[c,f]	40	60[j]	1,544	618	926
	ST: 2.60[f]													
Back proj.		24,540[h]	24.8[h]	6,080[h]	10[s]	58	0	42	0[a,c,f]	92	8[a]	608	559	49
PV+ basket	ML: 1.04[f]	46,180[f]	22.6[f]	10,440[f]	pyr.: 11[k]					99	1[c,f]	1,014	943	71
	ST: 1.19[f]				inrn.: 1[f]									
Bistrati-fied	ML: 2.09[f]	76,040[f]	21.0[c]	15,970[c,f]	10[g]	51	7	42	0[c,f,m]	92	8[a]	1,597	1,469	128
	ST: 1.86[f]													
Axo-axonic	0.60[n]			7,200[a,c,n]	6[c,n]	0	100	0	0[a]	100	0[n,r]	1,200	1,200	0
	0.85[n]													
CCK+ basket	PD: 1[l]			10,000[c,l]	8[k]	19	60	20	1[m]	92	8[a]	1,250	1,150	100
SCA	PD: 1.1[l]			12,000[a,c,l]	6[l]	10	4	82	4[c,l,p]	92	8[a]	2,000	1,840	160

Cell	Axonal			Classical Boutons		Laminar Distribution (%)				Divergence				
	Extent	Length	Density							Fraction (%)		Connections		
	(mm)	(μm)	(/100 μm)	Total	Syn.s /conn	SO	SP	SR	SLM	Pyr.	Inrn.	Total	Pyr.	Inrn.
PPA				8,000[a,c,l]	6[l]	0	0	0	100[a]	92	8[a]	1,333	1,227	106

ML: medio-lateral, ST: septo-temporal, PD: proximo-distal, RC: rostro-caudal. Proj: projection. The subscripts are as follows:

[a] assumed;

[c] further calculations applied to assumed or referenced data;

[d] Fuentealba et al. (2010);

[e] Fuentealba et al. (2008a);

[f] Sik et al. (1995);

[g] Klausberger et al. (2004);

[h] Sik et al. (1994);

[i] Jinno et al. (2007);

[j] Ferraguti et al. (2004);

[k] Foldy et al. (2010);

[l] Vida et al. (1998);

[m] Pawelzik et al. (2002);

[n] Li et al. (1992);

[o] Katona et al. (1999a),

[p] Szabo et al. (2012),

[q] Tamas et al. (2003);

[r] Buhl et al. (1994b);

[s] Maccaferri et al. (2000);

[t] Szabadics and Soltesz (2009);

[u] Armstrong et al. (2011);

[v] Takacs et al. (2008).

Table 6

Total number of synapses and ratio of GABA− to GABA+ synapses for various cell types by marker (Gulyas et al., 1999; Matyas et al., 2004; Takacs et al., 2008). The calculated number of each interneuron class is also given. We calculated the average number of GABA− and GABA+ synapses per interneuron, weighting the average by the total number of cells in each class.

Marker	Cells included*	Total cells	Synapses	
			GABA−	GABA+
PV	All three types	9,200	15,322	978
CCK	CCK+ basket	3,600	5,248	2,952
CR	IS I, III	6,190	1,738	462
n/a	Hippocampal-septal	950	18,920	3,080
Weighted Average			**9,461**	**1,274**

*We used the reported laminar distributions of the dendrites of the cells in each class to determine which interneurons were included in that class (Gulyas et al., 1999; Matyas et al., 2004; Takacs et al., 2008). n/a: not applicable.

Table 7

Distribution of COUP-TFII expressing cells by layer. The percent of COUP-TFII expressing cells found in each layer is listed, as well as the number of cells assuming a basis of 16,500 COUP-TFII expressing cells. Percentages from Fuentealba et al. (2010), see their suppl. fig. 1A.

Layer	% cells	Total cells
stratum lacunosum-moleculare	29%	4,790
stratum radiatum	22%	3,630
stratum pyramidale	35%	5,780
stratum oriens	14%	2,310
Total COUP-TFII+ cells	**100%**	**16,500**

Table 8

Percentage of NPY+ cells expressing nNOS (Fuentealba et al., 2008a, 2010). For each assay included, the calculations were made by summing all combinations including nNOS and NPY, and dividing that number by the sum of all combinations including NPY. Though the assays included other markers (listed in column 1), the calculation process was the same for each assay.

Assay	Total (%)	Laminar Expression (%)				Ref.
		SO	SP	SR	SLM	
nNOS/NPY/CB	81.0					Fuentealba et al. (2008a), Table S2
nNOS/NPY/CR	93.3					Fuentealba et al. (2008a), Table S2
nNOS/NPY/SOM	80.3					Fuentealba et al. (2008a), Table S2
nNOS/NPY/α-actinin-2	87.6					Fuentealba et al. (2008a), Table S2
nNOS/reelin/NPY/SOM	73.6	44.8	81.7	91.0	55.2	Fuentealba et al. (2010), Suppl. Table 2
NPY/COUP-TFII/nNOS	78.1	63.0	78.3	87.4		Fuentealba et al. (2010), Suppl. Table 2
PV/nNOS/NPY	56.7	34.7	54.2	88.9	41.2	Fuentealba et al. (2008a), Table S1
PV/nNOS/NPY/$GABA_A$R-α1	79.4	94.8	74.2	93.5	85.4	Fuentealba et al. (2008a), Table S2

Table 9

Laminar distribution of ivy cell boutons. Both studies used Sprague-Dawley rats.

Layer (%)				Ref.	Somata Layers
SO	SP	SR	SLM		
75	0	25	0	Fuentealba et al. (2008a)	Pyramidale
6	3	75	16	Szabo et al. (2012)	Pyramidale, Radiatum
40	2	50	8	Average	

Table 10

Laminar distribution of SOM within the CA1.

Layer (%)				Ref.	Notes
SO	**SP**	**SR**	**SLM**		
85.0	7.0	8.0		Nomura et al. (1997b)	Dorsal
92.0	3.0	5.0		Nomura et al. (1997b)	Ventral
88.5	5.0	6.5		Nomura et al. (1997b)	Averaged[1]
88.0	9.1	2.9		Kosaka et al. (1988)	Dorsal
89.8	6.8	3.4		Kosaka et al. (1988)	Ventral
89.0	7.9	3.1		Kosaka et al. (1988)	Dorsal+Ventral
89.7	7.3	2.5	0.5	Jinno and Kosaka (2006)	Mouse
73.3	22.8	3.9	0.0	Fuentealba et al. (2010)	Calculated

Note that data from Nomura et al. (1997b) and Kosaka et al. (1988) combine the strata radiatum and lacunosum-moleculare.

[1]Calculated average of the dorsal and ventral values.

Table 11

Laminar distribution of PV+ cells within the CA1. Note that data from Nomura et al. (1997b) and Kosaka et al. (1987) combine the strata radiatum and lacunosum-moleculare.

Layer				Ref.	Notes
SO	SP	SR	SLM		
36.0%	60.0%	4.0%		Nomura et al. (1997b)	Dorsal
24.0%	69.0%	7.0%		Nomura et al. (1997b)	Ventral
30.0%	64.5%	5.5%		Nomura et al. (1997b)	Averaged[1]
40.7%	54.9%	4.5%		Kosaka et al. (1987)	Dorsal
39.4%	52.8%	7.9%		Kosaka et al. (1987)	Ventral
40.0%	54.0%	6.0%		Kosaka et al. (1987)	Dorsal+Ventral
28.4%	64.5%	6.2%	0.9%	Jinno and Kosaka (2006)	Mouse

[1]Calculated average of the dorsal and ventral values.

Table 12

Relative proportion and number of each type of PV+ cell in the CA1. Cell type percentages are from Baude et al. (2007) and laminar distribution percentages are averaged from dorsal and ventral data in Nomura et al. (1997b).

		Layer			Total Cells
		SO[1]	SP	SR	
Cell type	**% cells**	**30.0%**	**64.5%**	**5.5%**	
PV+ basket cells	60.0%	1,320	3,880	330	5,530
Bistratified cells	24.0%	530	1,550	130	2,210
Axo-axonic cells	16.0%	350	1,030	90	1,470
Total PV+ cells[1]		**2,200**	**6,460**	**550**	**9,210**

Note that the percentage reported to be in the strata radiatum/lacunosum-moleculare is here attributed to the stratum radiatum only, as PV distribution data from the mouse showed that the stratum lacunosum-moleculare contained less than 1% of PV+ cells (Jinno and Kosaka, 2006, in mouse). 'Total PV+ cells' refers to PV+ basket, bistratified, and axo-axonic cells only.

[1]A fraction of PV+ O-LM and double projection cells was subtracted from the total PV+ cells in the stratum oriens before calculating the number of PV+ basket, bistratified, and axo-axonic cells in that layer.

Table 13

Laminar distribution of bistratified cell boutons.

Layer (%)				Ref.	Somata Layers
SO	SP	SR	SLM		
42	6	52	0	Pawelzik et al. (2002)	Pyramidale
53	14	33	0	Pawelzik et al. (2002)	Oriens
58	0	42	0	Sik et al. (1995)	Oriens
51	7	42	0	Average	

Table 14

Laminar distribution of CCK within the CA1. Note that data from Kosaka et al. (1985) combine the strata radiatum and lacunosum-moleculare. Methods A and B are described in the original paper, see Kosaka et al. (1985).

Layer (%)				Ref.	Notes
SO	SP	SR	SLM		
16.1	17.7	66.3		Kosaka et al. (1985)	Method A
18.8	19.7	61.6		Kosaka et al. (1985)	Method B
21.3	20.0	36.5	22.2	Pawelzik et al. (2002)	
22.6	29.2	39.1	9.2	Jinno and Kosaka (2006)	Mouse

Table 15

Calculated number of each type of CCK+ cell in the CA1. Based on laminar distribution percentages from Pawelzik et al. (2002) and marker coexpression fractions from Somogyi et al. (2004).

	Layer				
Cell Type	**SO**	**SP**	**SR**	**SLM**	**Total**
CCK+ Basket	**780**	**940**	**1,170**	**710**	**3,600**
VIP	310	240	80	50	680
VGLUT3	140	170	820	500	1,630
CCK only	330	530	270	160	1,290
SCA	**0**	**0**	**400**	**0**	**400**
CB	0	0	260	0	260
VGLUT3	0	0	0	0	0
CCK only	0	0	140	0	140
ADI	**0**	**0**	**390**	**0**	**390**
CB	0	0	250	0	250
VGLUT3	0	0	0	0	0
CCK only	0	0	140	0	140
PPA	**0**	**0**	**0**	**490**	**490**
CB	0	0	0	310	310
VGLUT3	0	0	0	0	0
CCK only	0	0	0	180	180
Misc CCK	**360**	**130**	**0**	**0**	**490**
CB	360	130	0	0	490
Total	**1,140**	**1,070**	**1,960**	**1,200**	**5,370**

Table 16

Laminar distribution of SCA cell boutons.

Layer (%)				
SO	**SP**	**SR**	**SLM**	**Ref.**
0	0.2	97.4	2.4	Vida et al. (1998)
19.2	8.2	67.4	5.2	Szabo et al. (2012)
9.6	4.2	82.4	3.8	Average

Table 17

Laminar distribution of CR and VIP within the CA1.

Marker	Layer (%)				Ref.	Notes
	SO	SP	SR	SLM		
CR+	22.0	38.0	40.0		Nomura et al. (1997b)	Dorsal
CR+	19.0	34.0	47.0		Nomura et al. (1997b)	Ventral
CR+	20.5	36.0	43.5		Nomura et al. (1997b)	Averaged[1]
CR+	14.1	45.2	24.8	15.9	Jinno and Kosaka (2006)	Mouse
CR+	19.7	46.8	16.9	16.6	Fuentealba et al. (2010)	Calculated[2]
CR+	18.8	38.7	12.6	29.9	Fuentealba et al. (2010)	Calculated[3]
VIP+	9.6	57.7	19.2	13.5	Jinno and Kosaka (2006)	Mouse
VIP+	6.0	42.4	19.7	31.9	Fuentealba et al. (2010)	Calculated[2]
CR+ or VIP+	14.6	41.4	18.5	25.5	Fuentealba et al. (2010)	Calculated[2]
CR+ and VIP−	21.9	40.6	17.5	20.0	Fuentealba et al. (2010)	Calculated[2]
CR+ and VIP+	13.9	63.6	15.2	7.4	Fuentealba et al. (2010)	Calculated[2]
CR− and VIP+	0.0	26.0	23.2	50.8	Fuentealba et al. (2010)	Calculated[2]

Note that data from Nomura et al. (1997b) combine the strata radiatum and lacunosum-moleculare.

[1] Average of the dorsal and ventral values.

[2] Calculated based on data from the marker assay: CR/COUP-TFII/PPE/VIP.

[3] Calculated based on data from the marker assay: CR/CB/COUP-TFII/PV.

Table 18

Calculated number of each IS cell type in the CA1 by layer.

Cell Type	Layer				Total
	SO	SP	SR	SLM	
IS I cells	780	1,800	780	890	4,250
IS II cells	0	480	450	1,040	1,970
IS III cells	0	910	220	120	1,250

Table 19

Number of GABA− and GABA+ synapses on pyramidal cell dendrites by layer and thickness of dendrite. Reprinted from Table 3 of Neuroscience, 102, Megias M, Emri Z, Freund T, Gulyas A, Total number and distribution of inhibitory and excitatory synapses on hippocampal CA1 pyramidal cells, 527–540, 2001, with permission from Elsevier. T: thick, M: medium, t: thin, dist: distal, med: medial, prox: proximal, Ori: stratum oriens, Rad: stratum radiatum, L-M: stratum lacunosum-moleculare

	Synapses		
Dendrite	**All**	**GABA−**	**GABA+**
Ori/dist	12,141	11,735	405
Ori/prox	479	246	233
Rad/T/prox	196	4	193
Rad/T/med	340	277	63
Rad/T/dist	2,219	2,171	48
Rad/t	14,862	14,425	437
L-M/T	565	486	80
L-M/M	493	418	76
L-M/t	1,051	873	179
Total	**32,351**	**30,637**	**1,713**

Table 20

Schaffer Collateral bouton counts per CA3 pyramidal cell based on a CA3a distribution (Sik et al., 1993) or a CA3c distribution (Wittner et al., 2007). The average of the CA3a and CA3c distributions and total bouton counts is also calculated. Lac. Mol.: lacunosum-moleculare.

	CA3a		CA3c		
Layer	**%**	**Boutons**	**%**	**Boutons**	**Average**
Lac. Mol.	0.0	0	0.4	110	55
Radiatum	20.8	3,181	94.2	25,848	14,515
Pyramidale	15.4	2,355	2.4	659	1,507
Oriens	63.8	9,758	3.0	823	5,291
Total		15,295		27,440	21,368

Table 21

Comparison of the total available excitatory synapses on a CA1 pyramidal cell with the calculated boutons available from the Schaffer Collateral path per CA1 pyramidal cell. The remaining “unclaimed” synapses left after subtracting the Schaffer Collateral inputs are also given. Because no dendrites were reported in the pyramidal layer (Megias et al., 2001), the boutons reported in the pyramidal layer were evenly divided between the stratum radiatum and stratum oriens. S. C.: Schaffer Collateral. Exc.: excitatory. Lac. Mol.: lacunosum-moleculare.

	Exc. Synapses on a CA1 Pyramidal Cell		
Layer	**Total**	**S.C. Inputs**	**Remaining**
Lac. Mol.	1,776	34	1,742
Radiatum	16,878	8,871	7,547
Pyramidale		921	
Oriens	11,982	3,233	8,288
Total	**30,636**	**13,059**	**17,577**

Table 22

Calculated convergence of excitatory synapses onto a CA1 pyramidal cell, based on observations of CA1 pyramidal cell dendrites from Megias et al. (2001). The lower end of the Schaffer Collateral range is based on the bouton counts from axonal fills of CA3 cells, while the upper end of the range is based on CA1 pyramidal cell synapse counts from Megias et al. (2001).

Input Type	Calculated Boutons/ CA1 Pyr. Cell.
Entorhinal Cortex via SLM	< 1,742
Schaffer Collaterals	13,059 − 28,697
Entorhinal Cortex via Alveus	<< 1,742
Local Collaterals	197

Table 23

Calculated convergence of interneurons onto a CA1 pyramidal cell. Note that several cell types are not included here, such as back-projection, radiatum-retrohippocampal, and more. The numbers in this table are based on Table 5 and the total number of cells from Table 4.

Cell Type	Total Cells	Boutons /Cell	Boutons			Boutons /Conn.	Convergence
			Total (M)	% on Pyr. Cells	/Pyr. Cell		
Ivy	8,810	16,200	142.7	92%	422	10	42
Neurogliaform	3,580	13,200	47.3	92%	140	10	14
O-LM	1,640	16,370	26.8	89%	77	10	8
Double proj.	760	6,080	4.6	92%	14	10	1
Oriens retrohipp.	640	6,080	3.9	96%	12	10	1
PV+ basket	5,530	10,440	57.7	99%	183	11	17
Bistratified	2,210	15,970	35.3	92%	104	10	10
Axo-axonic	1,470	7,200	10.6	100%	34	6	6
CCK+ basket	3,600	10,000	36.0	92%	106	8	13
SCA	400	12,000	4.8	92%	14	6	2
PPA	490	8,000	3.9	92%	12	6	2
Total per pyr. cell				**Inhibitory synapses**	**1,118**	**Convergence**	**116**

Note that the total inhibitory synapses value here represents the number of input synapses for which the inputs have been determined here, not the total number observed as in Megias et al. (2001).

Table 24

Calculated convergence of interneurons onto a CA1 pyramidal cell by layer and dendrite type, in terms of number of synapses received. For some interneuron types, no data were available but the likely locations of their synapses are marked with an asterisk. Other interneuron types are not shown in this table. The 'Total Available' column values are based on the synapse counts on an average CA1 pyramidal cell from Megias et al. (2001). The 'Total Claimed' column gives the counts for the presynaptic cell types we have calculated in this assessment, and the 'Total Remaining' column gives the number of synapses remaining on the average pyramidal cell after subtracting the estimated innervation calculated in this assessment.

	Oriens		Radiatum						
Cell Type	**Distal**	**Proximal**	**Thick prox.**	**Thick dist.**	**Thin**	**LM**	**Soma**	**Axon**	**Total Boutons**
Ivy	169	4	4		211	34			422
Neurogliaform					24	116			140
O-LM	5					72			77
Double proj.	8				6				14
Oriens retrohipp.	7				5				12
PV+ basket		61	61				61		183
Bistratified	53	3	4		44				104
Axo-axonic								34	34
CCK+ basket		37	37			1	31		106
SCA	1	0	0		12	1			14
PPA						12			12
Synapse Summary									
Total Available	405	233	193	111	437	335	92	34	1,840
Total Claimed	243	105	106	0	302	236	92	34	1,118
Total Remaining	162	128	87	111	135	99	0	0	722
Percent Remaining	40%	55%	45%	100%	31%	30%	0%	0%	39%

Table 25

Total number of synapses and ratio of GABA- to GABA+ for various cell types by marker (Gulyas et al., 1999; Matyas et al., 2004; Takacs et al., 2008).

Marker	Total Synapses	% GABA+	Non GABAergic	GABAergic
PV	16,300	6%	15,322	978
CCK	8,200	36%	5,248	2,952
CB	3,800	29%	2,698	1,102
CR	2,200	21%	1,738	462
HS *	22,000	14%	18,920	3,080

* Hippocampal-septal cells, classified by their projection target rather than a marker expressed.

Table 26

Calculated convergence of excitatory synapses onto a hypothetical average interneuron in the CA1. There are also inputs from the entorhinal cortex via the alveus, as well as from other afferents.

Input Type	**Calculated Boutons/ Hypoth. Avg. Interneuron**
Entorhinal Cortex via Stratum Lacunosum-Moleculare	<1,394
Schaffer Collaterals	7,952 – 17,476
Local Collaterals	2,211
Total	**11,557 – 21,081**

Table 27

Convergence of interneurons onto an average interneuron. Because interneuron dendrites generally don't span all layers and because there is some selectivity among interneuron-interneuron connections, these numbers are not representative of any one interneuron. Rather, each interneuron is expected to receive inputs from only a subset of those listed above and may receive significantly more boutons and have a higher convergence from those types than the values listed here. Also note that the GABAergic inputs from the IS I, II, and III cell types and the GABAergic afferents are not included here.

Cell Type	Total Cells	Boutons /Cell	Boutons			Boutons /Conn.	Convergence
			Total (M)	% on Interneurons	/Interneuron		
Ivy	8,810	16,200	142.7	8%	297	10	30
Neurogliaform	3,580	13,200	47.3	8%	98	10	10
O-LM	1,640	16,880	26.8	11%	77	10	8
Double Projection	760	6,080	4.6	8%	10	10	1
Oriens retrohipp	640	6,080	3.9	4%	4	10	1
CB- septal proj.	190	6,080	1.2	100%	30	10	3
PV+ Basket	5,530	10,440	57.7	1%	10	1	10
Bistratified	2,210	15,970	35.3	8%	73	10	7
CCK+ Basket	3,600	10,000	36.0	8%	75	8	9
SCA	400	12,000	4.8	8%	10	6	2
PPA	490	8,000	3.9	8%	8	6	1
Total per hypoth. Avg. interneuron				**GABAergic synapses**	**692**	**Convergence**	**82**